

Supplementary Information for

Homologous recombination deficient mutation cluster in tumor suppressor *RAD51C* identified by comprehensive analysis of cancer variants

Rohit Prakash^{1,*,#}, Yashpal Rawal^{2,*}, Meghan R. Sullivan^{3,*}, McKenzie K. Grundy³, H el ene Bret⁴, Michael J. Mihalevic³, Hayley L. Rein³, Jared M. Baird³, Kristie Darrah³, Fang Zhang^{1,5}, Raymond Wang¹, Tiffany A. Traina⁶, Marc R. Radke⁷, Scott H. Kaufmann⁸, Elizabeth M. Swisher⁷, Rapha el Gu erois⁴, Mauro Modesti⁹, Patrick Sung², Maria Jasin^{1,#}, Kara A. Bernstein^{3,#,^}

Co-corresponding authors: Rohit Prakash, Maria Jasin, Kara Bernstein

Email: rohitpraka@gmail.com, m-jasin@ski.mskcc.org, karab@pitt.edu

This PDF file includes:

Supplemental Materials and Methods
Figures S1 to S8
Tables S1 to S5
SI References

Other supplementary materials for this manuscript include the following:

Tables S6

Supplemental Materials and Methods

Mutational predictive analysis through PolyPhen-2, SIFT, and PROVEAN

Polymorphism Phenotyping version 2 (PolyPhen-2), Sorting Intolerant From Tolerant (SIFT; RRID:SCR_012813), and Protein Variation Effect Analyzer (PROVEAN; RRID:SCR_002182), were used to predict the functional effects of the amino acid substitution for each variant. Variants with PolyPhen-2 scores ≥ 0.957 is considered probably damaging, while < 0.957 is considered possibly damaging or benign (1). In SIFT, variants with a binary cutoff of < 0.05 is damaging, while ≥ 0.5 is tolerated (2). Variants with PROVEAN scores ≤ -2.5 are considered deleterious, while > -2.5 are considered neutral (3, 4). To coalesce the results from all three tools, a binary number system was used to reclassify the scores. Variants predicted to “probably damaging”, “damaging”, or “deleterious” were given a score of 1 while variants predicted to be “benign”, “possibly damaging”, “tolerated” or “neutral” were given a score of 0. Binary scores from each of the predictive algorithms were added together to calculate a total predictive score.

Cell Lines Used

The cell lines used in this study are MCF10A and U2OS. U2OS and MCF10A RAD51C mutant cell line derivatives were authenticated using STR DNA profiling as described (5). The U2OS RAD51C mutant cell line is available at the Leibniz Institute DSMZ, German Collection of Microorganisms and Cell Culture.

MCF10A clonogenic assays and HR analysis

MCF10A *RAD51C* conditional cells (5), which contain an integrated DR-GFP reporter (6), were grown in DMEM HG/F-12 supplemented with 5% horse serum, 1% penicillin and streptomycin, 100 ng/ml cholera toxin, 20 ng/ml epidermal growth factor, 0.01 mg/ml insulin, and 500 ng/ml hydrocortisone at 37°C with 5% CO₂ atmosphere. RAD51C-WT and variants were generated in the conditional MCF10A cells as described, using lentiviral transduction of pRP6 vectors (RRID:Addgene_51740), which were derived from pWZL-hygro (5). Cells were seeded at 100,000 cells per well in a 6-well plate 24 hours before infection. The next day, cells were treated with self-deleting Lenti-Cre, as described (6). The following day virus was removed, cells were washed with PBS and incubated another 24 hours in MCF10A media before use.

For clonogenic survival, cells were seeded at 1000 or 2000 cells on 10-cm dishes 48 hours after Lenti-Cre transduction. Cells were incubated for 10 days and fixed in 100% methanol. Plates were stained with Giemsa, and colonies were counted. For genotyping post-Cre expression, colonies were transferred from a 10-cm plate into a 96-well plate and then expanded in a 24-well plate. Genomic DNA was extracted from cells in 24-well plates. PCR was performed for the LoxP flanked *RAD51C* at the *AAVS1* locus with the following primers: Oligo4, 5'ATTGTGCTGTCTCATCATTTTGGC (forward) (6); HR-3R, 5'CTGGGATACCCCGAAGAGTG (reverse) (7). Expected PCR product sizes are ~2.5 kb before Cre expression and ~1.3 kb after Cre deletion.

For HR analysis after Cre expression, 50,000 cells per well were seeded in 24-well plates. The next day, cells were infected with an I-SceI-expressing lentivirus (6), and two days later, GFP positive cells were measured by flow cytometry (BD FACScan). Data were analyzed using FlowJo software (FlowJo, RRID:SCR_008520). Without I-SceI expression, the number of GFP positive cells was $\leq 0.01\%$.

U2OS cell culture, HR analysis, and clonogenic survival

RAD51C mutant U2OS cells with an integrated SCR reporter (5) were cultured at 5% CO₂ in DMEM supplemented with 10% fetal bovine serum with 1% penicillin and streptomycin. For HR assays, 2 million cells were nucleofected with 1 μ g each plasmids expressing I-SceI (pCBASceI, Addgene plasmid # 26477, RRID:Addgene_26477; (8)) and wild-type or variant *RAD51C* (pRP6, derived from pWZL-hygro; RRID:Addgene_19834; (5)). *RAD51* focus formation was done blinded using cells stably expressing *RAD51C* variants from pWZL-*RAD51C* lentivirus, as described previously (5).

For clonogenic survival, *RAD51C* variants were expressed from pCMV-2B FLAG tagged plasmids that were stably integrated in cell pools selected in G418 for two weeks. Cells were seeded at 600 cells on 60mm in triplicate and treated 24 hours after plating with cisplatin or olaparib. For cisplatin, cells were exposed for 1 cell cycle as determined for each variant by doubling time calculations. For Olaparib, cells were exposed (Selleck Chem, AZD2281) continuously, replacing the media with fresh drug every 3 days. Cells were grown for 12-14 days, and fixed in 100% methanol. Plates were stained with crystal violet and scanned on a FluorChem M (proteinsimple).

U2OS Western blotting

XRCC3 was cloned (EcoR1/Sal1) into pCMV3B (MYC) and *RAD51C* was cloned (EcoR1/Sal1) into pCMV2B (FLAG). For Western blotting, pCMV3B-XRCC3 was co-transfected with pCMV2B-*RAD51C* variants or pCMV2B empty vector. Cells were harvested 24 hours later (~80% confluence) and lysed in NP-40 lysis buffer (50 mM Tris base, 100 mM NaCl, 2 mM MgCl₂, 10% glycerol, 0.1% NP-40) supplemented with 2 mM PMSF, protease inhibitor cocktail (A32965, Pierce), and phosphatase inhibitor cocktail (A32957, Pierce). Lysed cells were treated with Benzonase (Millipore Sigma, 70746) on ice for 20 min to eliminate DNA-mediated protein-protein interactions. Lysates were cleared by centrifugation and 10% volume was loaded on a 10% SDS-PAGE gel run at 80 V. Protein was then transferred onto PVDF membrane (Immobilon-FL, Millipore) at 100 V for 2 hours and blocked for 1 hour with Odyssey blocking buffer (Licor, 927-50000). Antibodies were diluted into Odyssey blocking buffer and Tris phosphate buffer (TBS) at a 1:1 ratio supplemented with 0.2% Tween-20. Antibodies included FLAG-M2 (Sigma, F3165; 1:2000) and GAPDH (Santa Cruz Biotechnology Cat# sc-25778, RRID:AB_10167668; 1:500). Secondary antibodies were all used at 1:20,000 and included Goat anti-Mouse IgG Light-Chain Specific for *RAD51C* (AlexaFluor 790-conjugated; Jackson ImmunoResearch Labs Cat# 115-655-174, RRID:AB_2338946) and IRDye680RD Goat anti-mouse (LI-COR Biosciences Cat# 926-68070, RRID:AB_10956588) for GAPDH. Membranes were then imaged using the LI-COR Odyssey CLx imaging system.

Yeast-two- and three-hybrids: plasmid construction and screening

Yeast-two-hybrid (Y2H) plasmids were created in pGAD-C1 and pGBD-C1 (RRID:Addgene_26735) for *RAD51B* (EcoRI/BglIII), *RAD51D* (EcoRI/Sall), and *XRCC3* (EcoI/Sall). The constitutively expressed yeast-three-hybrid (Y3H) plasmid was created in pRS-ADH-416 for *RAD51B* (EcoRI/Sall). *RAD51C* mutant vectors were made by sub-cloning *RAD51C* into the pGAD-C1 or pGBD-C1 vectors using 5'EcoRI and 3'Sall restriction sites. Specific point mutations were introduced by site-directed mutagenesis of the pGAD-*RAD51C* or pGBD-*RAD51C* vectors. *RAD51C* cDNA and *RAD51B* cDNA were a gift from Jun Huang, *RAD51D* cDNA was a gift from Paul Russell, and pGAD-*XRCC3* and pGBT-*XRCC3* plasmids were a gift from David Schild.

Y2Hs and Y3Hs were performed as described in (9) except that the pGAD, pGBD, and pRS-ADH-416 plasmids were co-transformed into the YPJ69-4a yeast strain. *RAD51C* variants were queried in both the pGAD and pGBD vectors for interaction with each binding partner by plating on synthetic complete medium (SC) without leucine, tryptophan, and histidine (SC-LEU-TRP-HIS), where growth is indicative of a Y2H interaction, SC without leucine, tryptophan, uracil, and histidine (SC-LEU-TRP-URA-HIS), where growth is indicative of a Y3H interaction, and loading controls SC without leucine and tryptophan (SC-LEU-TRP) for the Y2H or SC without leucine, tryptophan, and uracil (SC-LEU-TRP-URA) for the Y3H, respectively. Images were identically adjusted for brightness and contrast in Adobe Photoshop (Adobe Photoshop, RRID:SCR_014199). Analysis was performed in duplicate or triplicate with fresh transformations for each biological replicate. Relative interaction of each *RAD51C* variant was quantified in ImageJ (ImageJ, RRID:SCR_003070) and normalized to wild-type *RAD51C* interactions (which was set to 100%) per plate. The corresponding empty vector was subtracted to adjust for background growth.

Correlations between HR, Y2H, and Y3H results were plotted in GraphPad Prism (GraphPad Prism, RRID:SCR_002798) relative to wild-type phenotypes with linear regressions (black) and 95% confidence intervals (green area). Pearson correlation statistical tests were used to calculate *r* values and were annotated on each graph.

Yeast-2-hybrid Western blots

Yeast expressing *RAD51C* wild-type or the mutant *RAD51C* expressed in the pGAD-C1 (AD expression vector) and *XRCC3* expressed in the pGBD-C1 (BD expression vector) was grown over night in YPD medium. Protein was lysed using TCA precipitation as described (10) and 0.75 OD₆₀₀ of total protein was analyzed by 10% SDS-PAGE gel. *RAD51C* protein and the loading control *Kar2* was detected on a LiCor CLX scanner. *RAD51C* and *XRCC3* expression was detected using *RAD51C* antibody (Abcam Cat# ab55728, RRID:AB_945135, 1:500), *XRCC3* antibody (Novus Cat# NB100-180B, RRID:AB_1849481, 1:2000), and *Kar2* Santa Cruz antibody (sc-33630, 1:2000) and LI-COR IRDye secondary antibodies (goat anti-mouse LI-COR Biosciences Cat# 926-68070, RRID:AB_10856588 for *XRCC3* at 1:20,000; donkey anti-mouse (LI-COR Biosciences Cat# 926-68072, RRID:AB_10953628 at 1:20,000 for *RAD51C*; and goat anti-rabbit LI-COR Biosciences Cat# 926-32211, RRID:AB_621843 at 1:20,000 for *Kar2*).

Purification of BCDX2 and CX3 complexes

Hi5 insect cells were infected for 48 hours with baculoviruses expressing BCDX2 (RAD51B-His and XRCC2-Flag) and CX3 (MBP-RAD51C and XRCC3-Flag) complexes with WT RAD51C or the indicated RAD51C mutant. All the purification steps were carried out at 0-4°C.

For BCDX2 purification, crude cell lysate was prepared from 6-8 g cell pellet (from 800 ml insect cell culture) by sonication in 50 ml T buffer (25 mM Tris-HCl, pH 7.5, 10% glycerol, 0.5 mM EDTA, 1 mM DTT, 0.05% IGEPAL, 20 mM imidazole, 1 mM PMSF and protease inhibitors) containing 300 mM KCl, 5 mM ATP, and 2 mM MgCl₂, followed by centrifugation at 100,000 Xg for 60 min. The clarified lysate was incubated with 2.5 ml Ni-NTA resin (Qiagen, 1018142) for 1 hour, followed by sequential washes of the resin with 25 ml T buffer with 300 mM KCl, 500 ml T buffer with 1000 mM KCl and 25 ml T buffer with 100 mM KCl and with all the buffer also containing 2 mM each of ATP and MgCl₂. The BCDX2 complex was eluted from the affinity matrix with 10 ml T buffer containing 200 mM imidazole and 2 mM each of ATP and MgCl₂. Further purification was by ion exchange in a 1 ml HiTrap Q HP column fractionated with a 30 ml 150-450 mM KCl gradient in T buffer. Peak fractions were pooled and concentrated to 0.4 ml in a Amicon 30 concentrator and then subject to size exclusion chromatography in a Superose 6 Increase 10/300 GL column in T buffer with 300 mM KCl and 2 mM each of ATP and MgCl₂.

Lysates containing CX3 complexes were prepared and clarified as described above. The clarified lysate was incubated with 2 ml amylose resin (NEB, E8021) for 2 h, followed by sequential washes of the resin with 25 ml T buffer with 300 mM KCl, 200 ml T buffer with 1000 mM KCl and 25 ml T buffer with 300 mM KCl and with all the buffers also containing 2 mM each of ATP and MgCl₂. CX3 complex was eluted from the affinity matrix with 10 ml T buffer containing 20 mM maltose and 2 mM each of ATP and MgCl₂. For further purification, the eluate from the amylose affinity step was incubated with 1 ml anti-FLAG M2 resin (Sigma, A2220) for 2 h, followed by washing with 50 ml T buffer containing 300 mM KCl and 2 mM each of ATP and MgCl₂ before protein elution with the same buffer containing 200 ng/μl FLAG peptide (Sigma, F3290). The eluate was concentrated to 0.4 ml and then fractionated by size exclusion in a Superdex 200 10/300 column in same buffer without the FLAG peptide. For cleaving the MBP tag, following the affinity purification step in the anti-FLAG resin, CX3 complexes were concentrated to 0.4 ml and incubated overnight with 100 μg of TEV protease. The CX3 complexes were separated from the cleaved MBP tag and TEV protease by fractionation on a Superdex 200 10/300 column as above.

DNA binding and ATPase assays

For DNA binding, 1 nM of 5' ³²P-labeled 80-nt ssDNA (11) was incubated with the indicated concentration of purified BCDX2 complex in 10 μl reaction buffer (50 mM Tris-HCl, pH 7.5, 155 mM KCl, 1 mM DTT, 1 mM ATP, 1 mM MgCl₂ and 100 μg BSA) for 10 min at 37°C. Nucleoprotein complexes were resolved on 5% polyacrylamide gels in Tris-borate buffer. Gels were dried and subjected to phosphorimaging analysis. BCDX2 complexes (2.0 μM) were incubated in the absence or presence of ssDNA (20 μM nucleotides, phiX174 virion) in 10 μl of reaction buffer (20 mM HEPES at pH 7.5, 1 mM DTT, 1 mM MgCl₂) containing 0.05 mM [γ-³²P] ATP at 37°C. Aliquots of 2 μl were withdrawn at the indicated times and mixed with 2 μl of 0.5 M

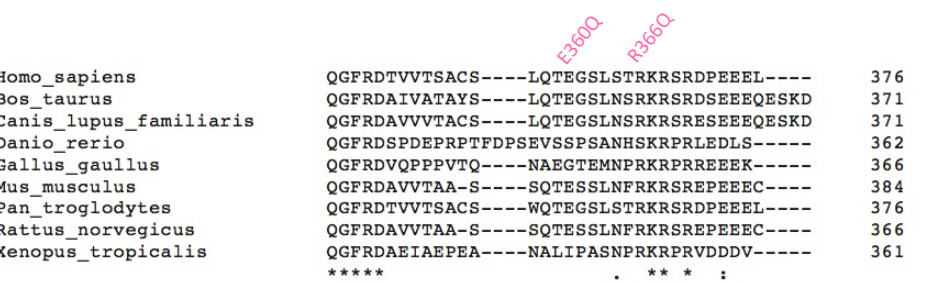
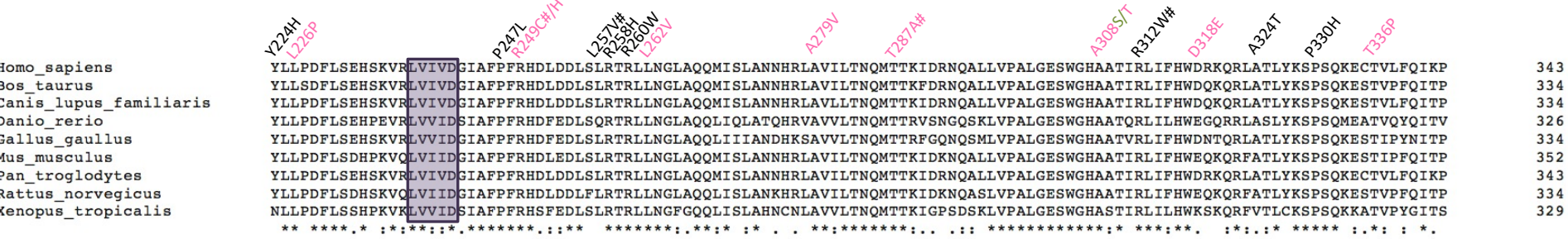
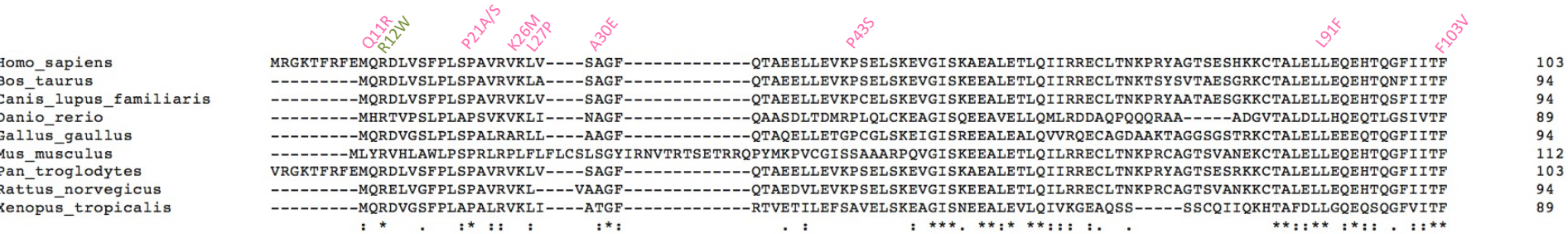
EDTA to stop the reaction. The level of ATP hydrolysis was determined by layer chromatography on PEI cellulose F sheets (Millipore, 105579) in 0.375 M potassium phosphate (pH 3.5).

Structural modeling of the BCDX2 and CX3 complexes

RAD51B, RAD51C, RAD51D, XRCC2 and XRCC3 sequences from UniProt database (RRID:SCR_004426 (12)) were used as input in the mmseqs2 homology search program (13) and a multiple sequence alignment (MSA) was generated against the UniRef30 clustered database (14). Only orthologs from the MSA of each paralog were selected. For this, homologs of RAD51B and RAD51C sharing less than 35% sequence identity with their respective query and those of XRCC2 and XRCC3 sharing less than 30% were discarded. Homologs with less than 50% of coverage of the aligned region of their query were also discarded. Next, all species having at least one homolog in the MSAs for every RAD51 paralog were selected; only the homolog with highest sequence identity to the query was kept. Full-length sequences of the orthologs were retrieved and re-aligned with mafft (15). MSAs of RAD51B, RAD51C, RAD51D, XRCC2 and MSAs of RAD51C, XRCC3 were concatenated matching the sequences of the same species resulting into two paired MSAs for the BCDX2 and CX3 complexes, respectively. Final concatenated MSAs contained 1368 and 722 positions and 384 and 714 sequences for BCDX2 and CX3, respectively. Both paired MSAs were used as inputs to generate 5 structural models for each of the BCDX2 and CX3 complexes, respectively, using a local version of the ColabFold interface (14) running 3 iterations of the AlphaFold2 algorithm v2.1.0 (16) trained on the multimer dataset (17) on a local HPC equipped with NVIDIA Ampere A100 80Go GPU cards. The five models for each complex converged toward very similar conformations and obtained high confidence and quality scores with pLDDTs in the range [79.1, 85] and [84.5, 88.1] and pTMscore in the range [0.75, 0.801] and [0.825, 0.846] for BCDX2 and CX3 complexes, respectively. The models with highest pTMscores for BCDX2 and CX3 models were relaxed using rosetta relax protocols to remove steric clashes (18) with strong backbone constraints (std dev. of 0.5 Å for the atomic positions) and were used for structural analysis. The solvent accessibility of every mutated residue was computed with Naccess (19). The nucleotides and ssDNA that are shown bound to the structural models of RAD51 paralogs in **Fig. 5** were deduced from the superimposition of these subunits with those of RAD51 in the PDB structure 5H1B. The models are available in ModelArchive (modelarchive.org) with the accession codes ma-a54ps (BCDX2) and ma-52hi1 (CX3).

Supplementary Figure 1

A.

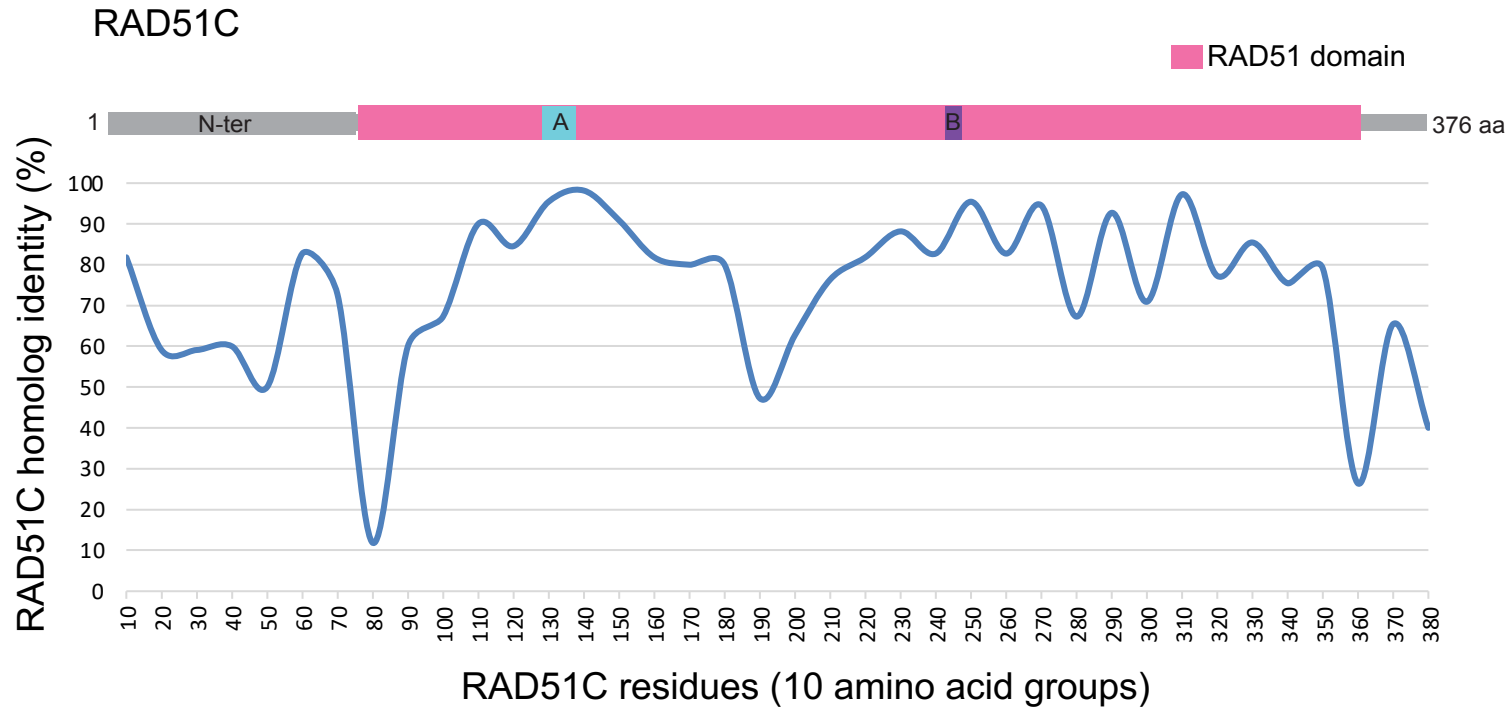


Clustal alignment:
 * fully conserved
 : strongly similar
 . weakly similar

Walker A motif (aa 125-132)
 Walker B motif (aa 238-242)

RAD51C variant code:
 Pink - BC/OC
 Black - other cancer
 Green - Population variant
 * Cancer mutation also identified as a population variant

B.



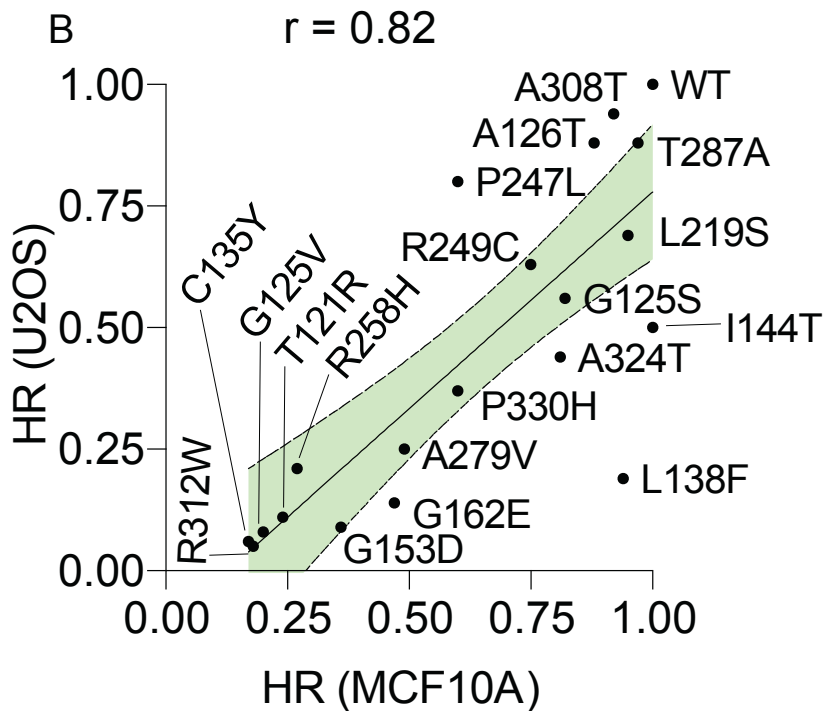
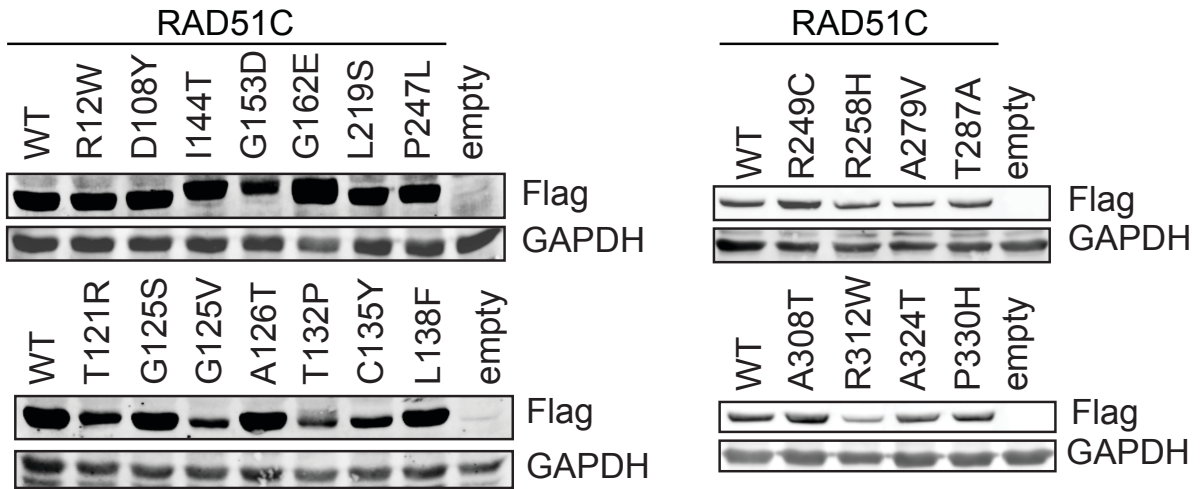
Supplementary Figure S1. RAD51C conservation among vertebrate species.

A. Clustal Omega was used to generate a multiple sequence alignment of RAD51C homologs from nine vertebrate species. Conserved residues are indicated with (*) for an invariant residue, (:) for strongly similar properties (roughly equivalent to scoring >0.5 in the Gonnet PAM 250 matrix: STA, NEQK, NHQK, NDEQ, QHRK, MILV, MILF, HY, FYW), or a (.) for weakly similar properties (roughly equivalent to scoring ≤ 0.5 and >0 in the Gonnet PAM 250 matrix: CSA, ATV, SAG, STNK, STPA, SGND, SNDEQK, NDEQHK, NEQHRK, FVLIM, HFY). RAD51C cancer (pink, BC/OC; black, other cancer) and population (green) variants are indicated. An asterisk indicates that the variant is found as both a cancer and population variant. Walker A and B motifs are indicated by blue and purple boxes, respectively.

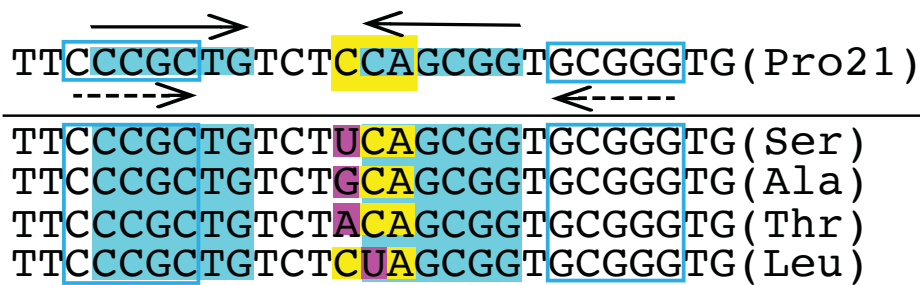
B. RAD51C homolog identity. The region around the Walker A box shows the highest level of identity although other well conserved regions are also observed. Jalview software was used to generate the identity in 10 amino acid bins, starting at amino acid 10 of human RAD51C since some of the homologs do not contain the first 9 residues.

Supplementary Figure S2

A



C



Supplementary Figure S2. Prediction algorithms have limited success for RAD51C HR function.

A. Western blotting for Flag-tagged RAD51C variants expressed in U2OS cells. A subset of variants with defective HR was chosen for analysis

B. Correlation of RAD51C variants for HR proficiency in MCF10A and U2OS cells. In both cell lines, HR levels are relative to that obtained with wild-type RAD51C. The linear regression is plotted in black with 90% confidence intervals shaded in green.

C. Four different variants are reported at RAD51C P21 in ClinVar, three of which have also been reported multiple times in cancers, including several breast cancers, such that P21 is considered a cancer hotspot. The CCA codon for P21 (yellow shading) is within a 6 bp GC rich inverted repeat (blue shading) and in between a 5 bp GC rich inverted repeat (blue outline), which could potentially make the sequence unstable, e.g., during DNA replication. The bp altered in the variant is highlighted (purple).

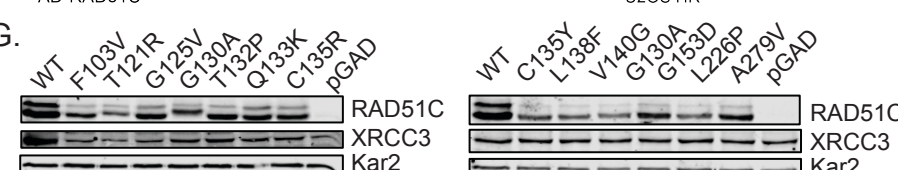
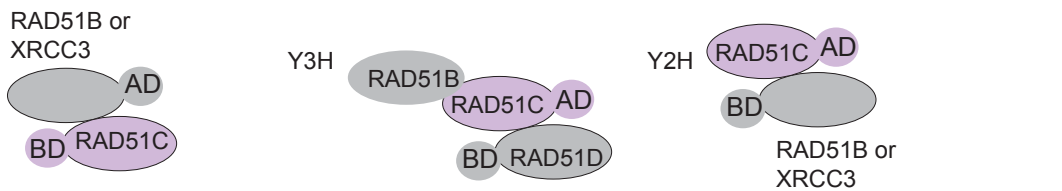
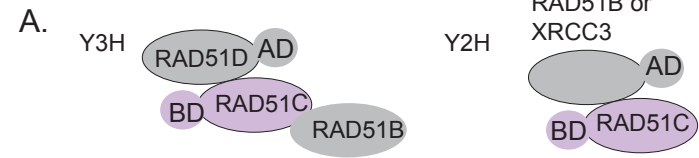


Figure 2

Supplementary Figure S3. RAD51C variant interactions with other RAD51 paralogs in Y2H/Y3H screens.

A. A yeast-two-hybrid (Y2H) approach was used to test interactions with RAD51B and XRCC3 and a yeast-three-hybrid (Y3H) approach was used for RAD51D, since RAD51C interaction is more robust in the presence of its binding partner RAD51B (20, 21). RAD51C variants were tested as both activating domain (AD) fusions (see **Fig. 2B**) and DNA binding domain (BD) fusions.

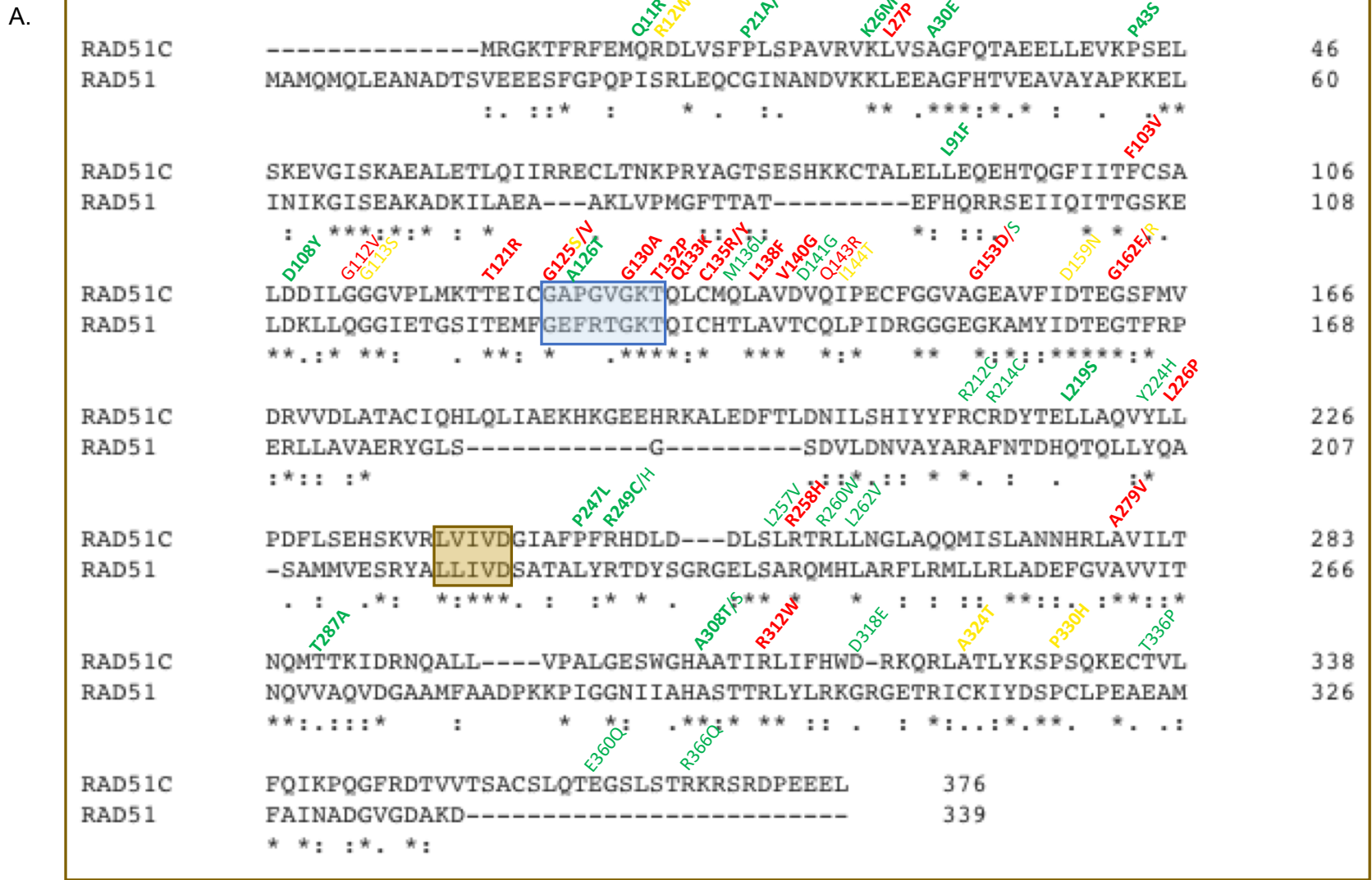
B. Representative Y2 and Y3H interactions of RAD51C variant BD fusions. Interaction is indicated by growth. Note: RAD51C P21S, G130A and D159N were not tested in the BD direction.

C. Heat map indicates averaged protein-protein interactions for the set of RAD51C mutants as determined by amount of growth in the Y2H/Y3H assays. RAD51C variant interaction with the indicated RAD51 paralog is relative to WT (green: 0.67-1.00, yellow: 0.34-0.66, red: 0-0.33). Growth was quantified using ImageJ from two or more independent experiments. The negative control was included on every plate (empty GAL4 BD plasmid).

D-F. Y2H/Y3H interactions for the RAD51C variants correlate in the AD versus BD directions for each of RAD51D (**D**), RAD51B (**E**), and XRCC3 (**F**) ($p < 0.001$ for each). Linear regression lines are shown in black with 90% confidence intervals shaded in green. Note that interaction results from the AD direction for T287A and D108Y correlate with HR (proficient in all directions; **Fig. 2C**), while the BD direction shows defective interactions with all paralogs.

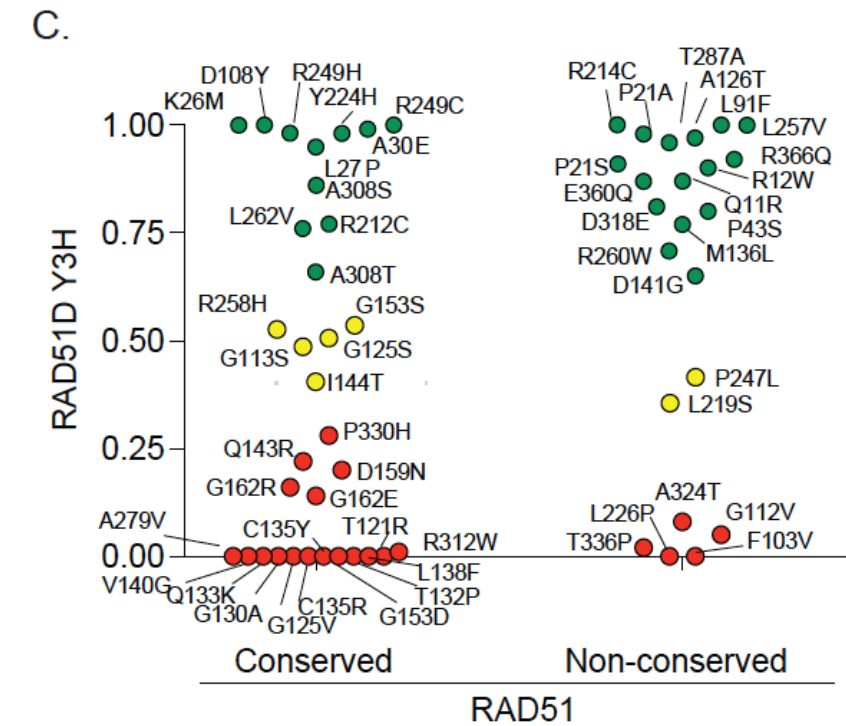
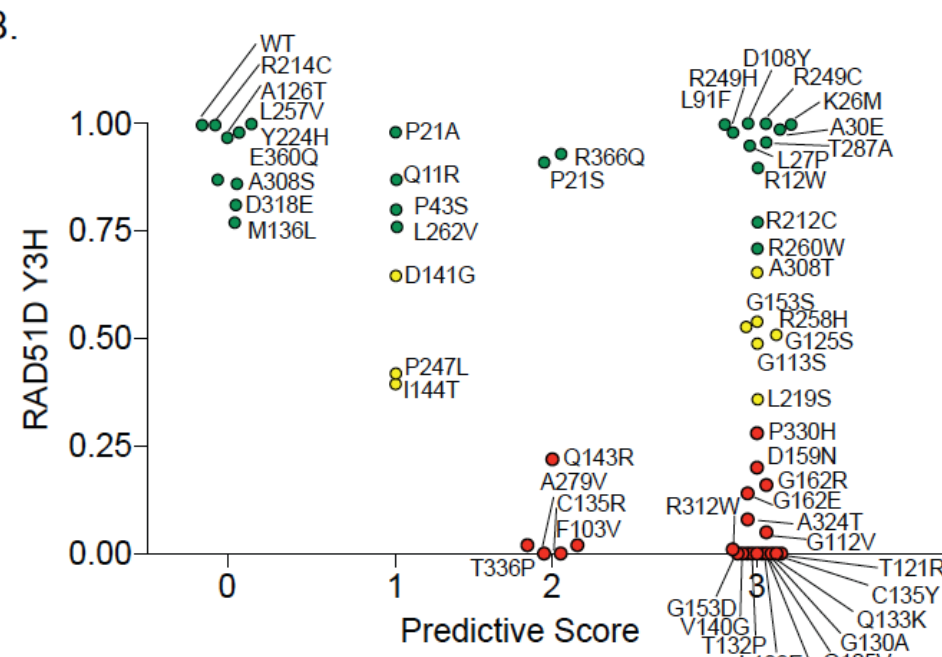
G. RAD51C variant expression in yeast. RAD51C variants were selected for Western blotting based on deficient interactions in Y2H/Y3H.

H-J. HR levels for the RAD51C variants correlate well with Y2H/Y3H interactions in the BD directions for each of RAD51D (**H**), RAD51B (**I**), and XRCC3 (**J**), with RAD51D interaction being the best predictor.

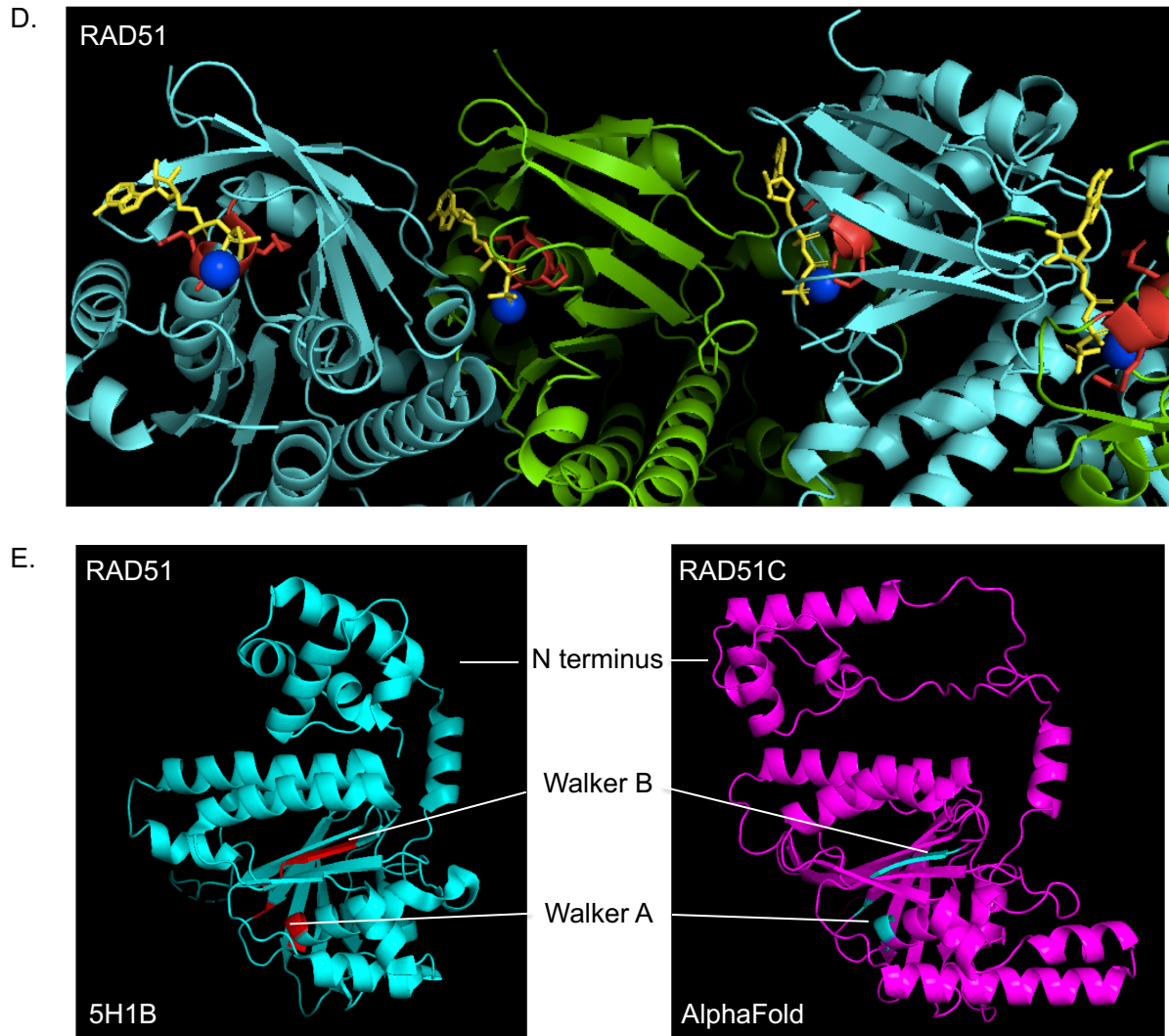


Conserved residues (*.): 27
 proficient 8 (30%)
 reduced 4 (15%)
 deficient 15 (55%)

Non conserved (..): 22
 proficient 17 (77%)
 reduced 2 (9%)
 deficient 3 (14%)



RAD51



Supplementary Figure S4. RAD51C has limited sequence identity with RAD51 but is predicted to be structurally well conserved.

A. RAD51C variants at conserved residues with RAD51 are much more likely to be critical for HR rather than nonconserved residues. The alignment (Clustal Omega) shows that the two proteins have only 28% protein sequence identity. RAD51C variants above the alignment are colored in bold according to their HR activity in U2OS cells (deficient HR, red; reduced HR, yellow; proficient HR, green); those not tested for HR are in regular type and are colored according to the Y2H/Y3H results. (See also lollipop diagram in **Fig. 4A**.) The Walker A and B boxes are shaded blue and purple, respectively.

B. Comparison of RAD51D interaction of the RAD51C variants by Y3H with the combined scores from the PolyPhen-2, SIFT, and PROVEAN prediction tools, as in **Fig. 3B**. The variants are colored according to whether RAD51D interaction is proficient (green), reduced (yellow), or deficient (red).

C. Comparison of RAD51C variant interaction with RAD51D with residue conservation with RAD51, as in **Fig. 3B**.

D. RAD51 filament structure demonstrating ATP near the interface of adjacent RAD51 monomers. Alternating monomers are in cyan and green, conserved Walker A motif residues in red, ATP in yellow, with the bound Mg²⁺ ion in blue. PDB: 5NWL (22).

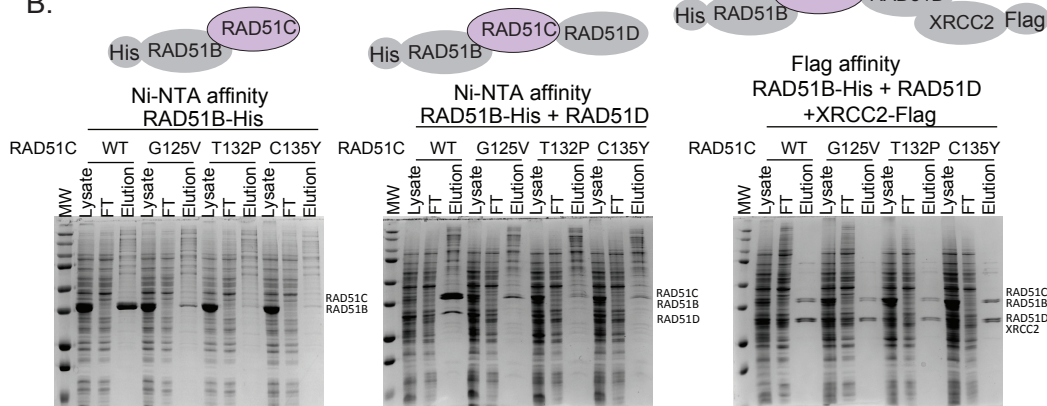
E. RAD51 and RAD51C are predicted to have similar structures. The Walker A and B motif residues, red in RAD51 and cyan in RAD51C, are similarly situated within the main globular fold. The RAD51 structure is from PDB: 5H1B (23), and the RAD51C structure prediction is from the AlphaFold Protein Structure Database (alphafold.ebi.ac.uk) (16). The N termini of the two proteins have structural similarity but are differently oriented; however, the linker between the two domains in RAD51C has a low confidence score in the structure prediction.

Supplementary Figure S5

A.

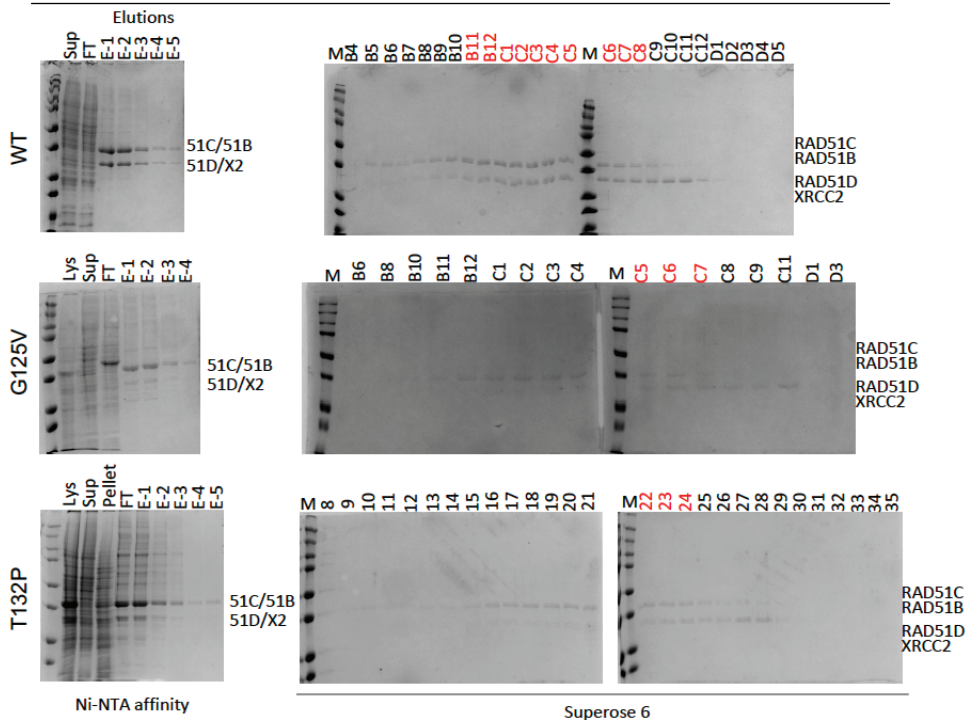
B.

BCDX2 complex purification scheme:
 (RAD51B-His
 RAD51C
 RAD51D
 XRCC2-Flag)
 Nickle affinity
 ↓
 HiTrap Q HP
 ↓
 Superose 6



C.

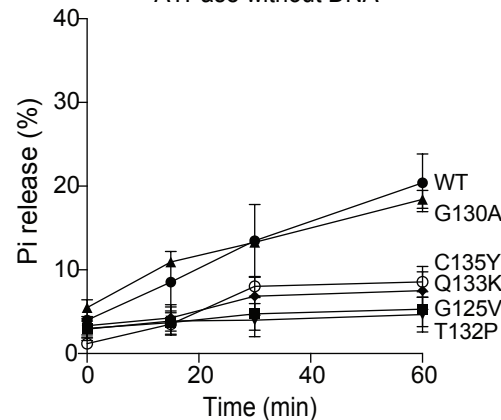
Purification of BCDX2 without ATP and MgCl₂



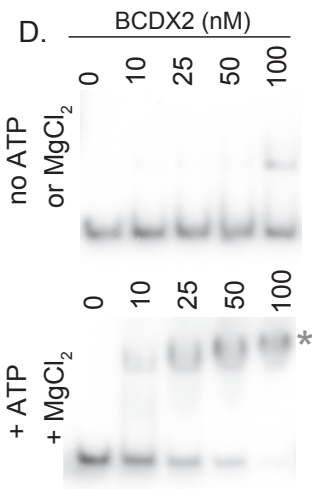
F.

RAD51C	Time	No DNA	With DNA
WT	60'	0.08503541	0.1320713
G125V	60'	0.022151	0.0241905
G130A	60'	0.07678847	0.09546789
T132P	60'	0.01940862	0.01717652
Q133K	60'	0.03139336	0.03424465
C135Y	60'	0.03563348	0.07237941

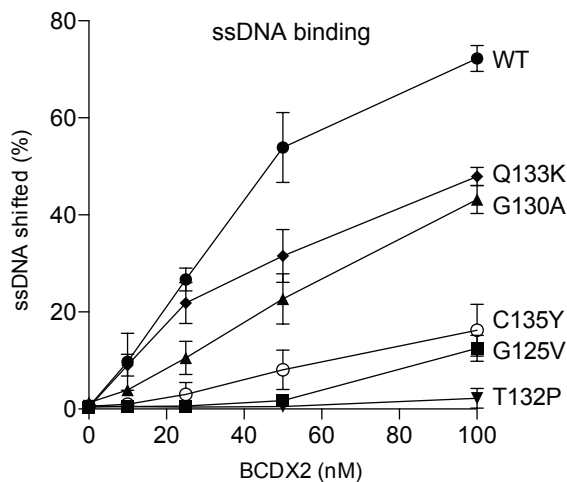
ATPase without DNA



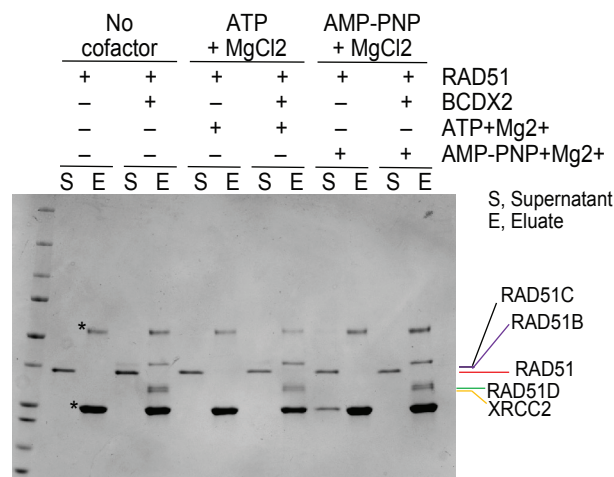
D.



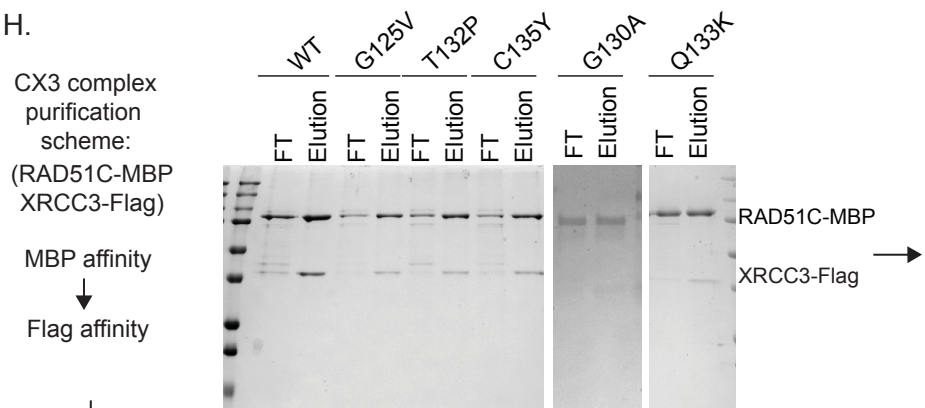
E.



G.



H.

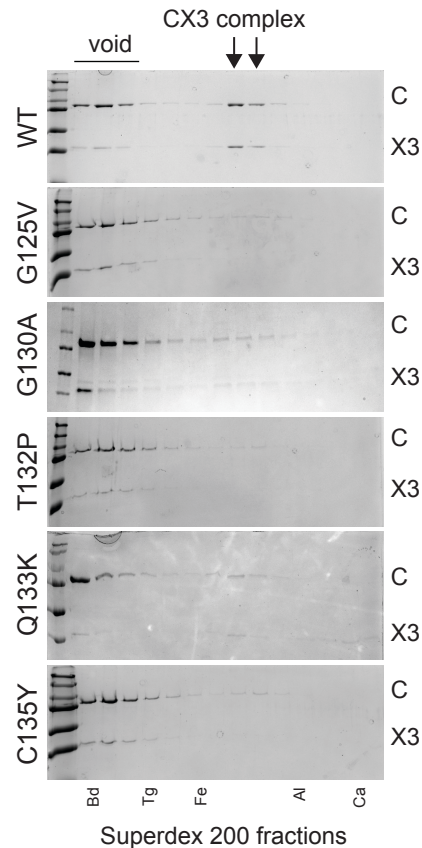
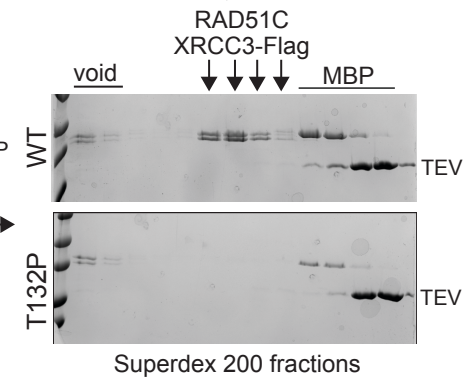
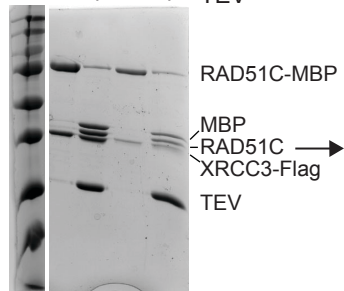


I.

TEV digestion

WT T132P

- + - + TEV



Supplementary Figure S5. Biochemical analysis of the RAD51C variants in the BCDX2 and CX3 complexes.

A. Purification scheme for BCDX2 complexes in the presence of ATP and MgCl₂. A three-step approach was used to purify BCDX2 complexes from insect cell extracts. The last step of the purification, fractionation on a Superose 6 column, is shown in **Fig. 4B**.

B. Wild-type RAD51C forms subcomplexes with RAD51B (BC, left) and RAD51B+RAD51D (BCD, middle), but the three RAD51C mutants are poor at subcomplex formation. However, they do form a complex when a fourth RAD51 paralog, XRCC2, is added (BCDX2, right). Experiments performed in the presence of ATP and MgCl₂

C. BCDX2 purified in the absence of ATP and MgCl₂ was less stable and frequently dissociated. Dissociation was more pronounced with the BC_{mut}DX2 complexes. Fractions containing all four paralogs are indicated in red.

D. ssDNA binding. ssDNA binding by the BCDX2 complex was assessed in the absence or presence of ATP and MgCl₂ by electrophoretic mobility shift assays using an 80mer substrate. DNA binding with ATP and MgCl₂ is indicated with an asterisk.

E. The graph shows ssDNA binding by the BCDX2 complexes as assessed by electrophoretic mobility shift assays in the presence of ATP and MgCl₂ using an 80mer substrate from three independent experiments.

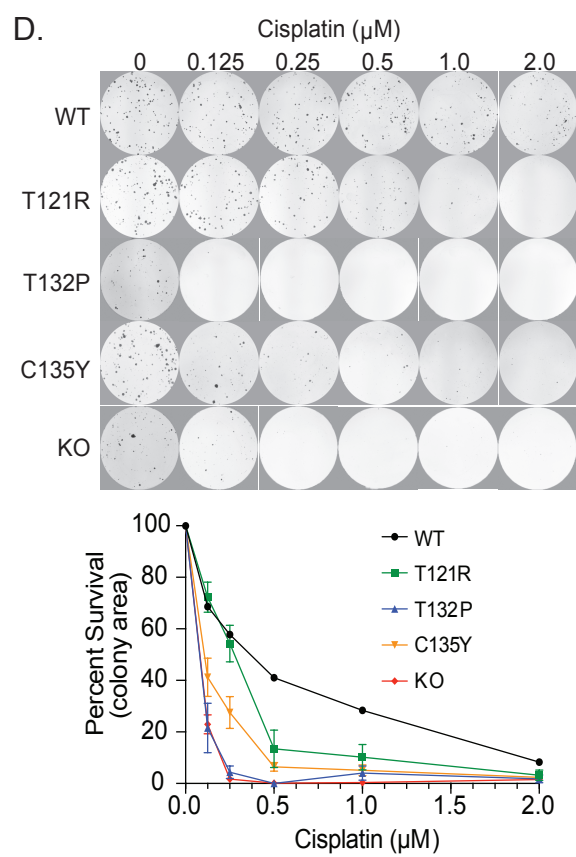
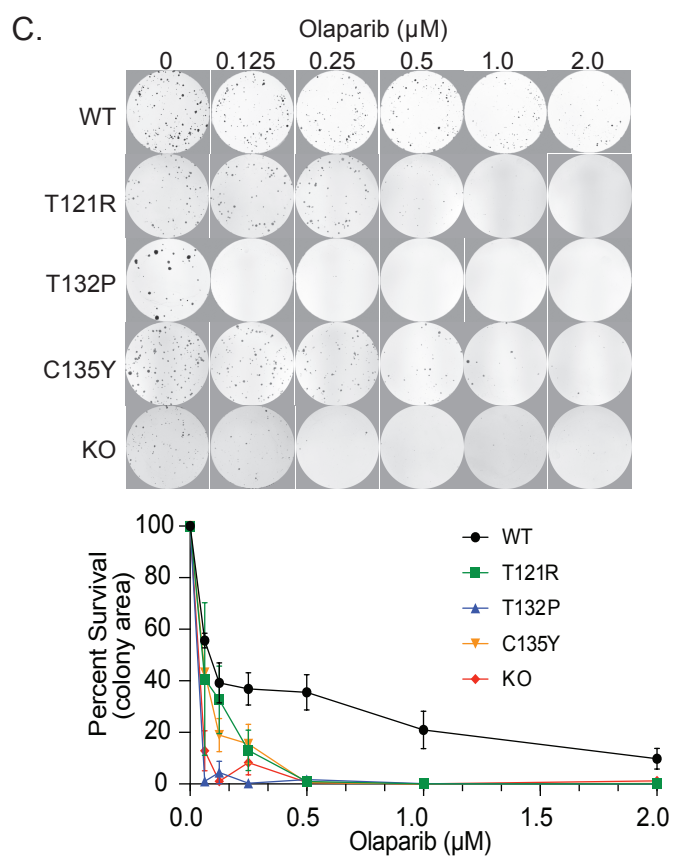
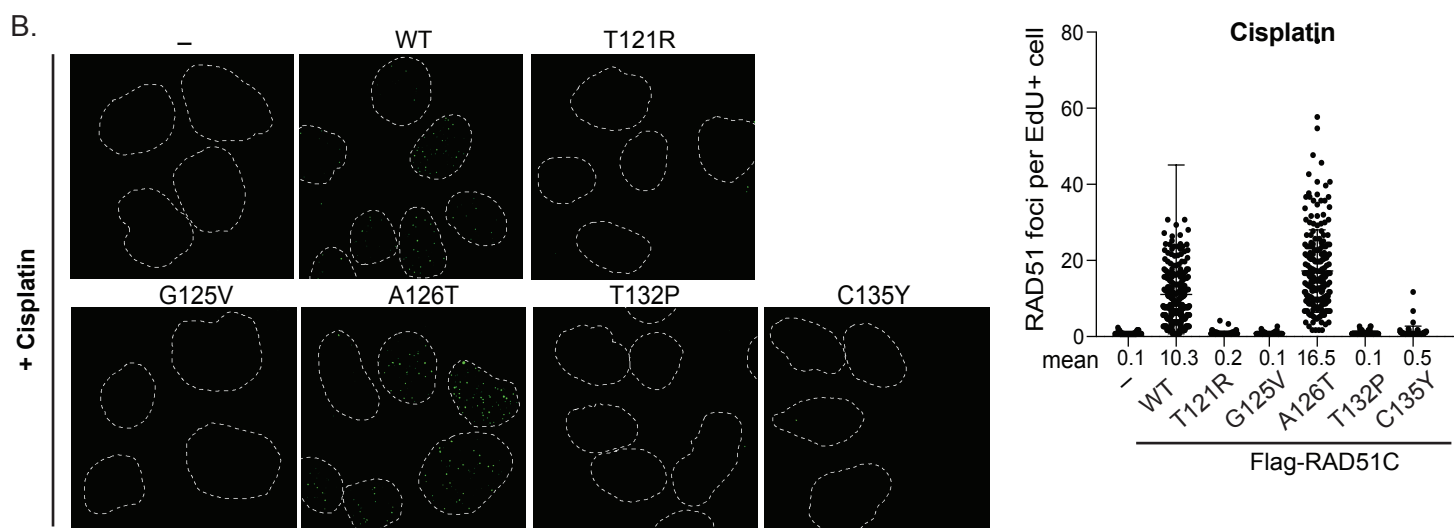
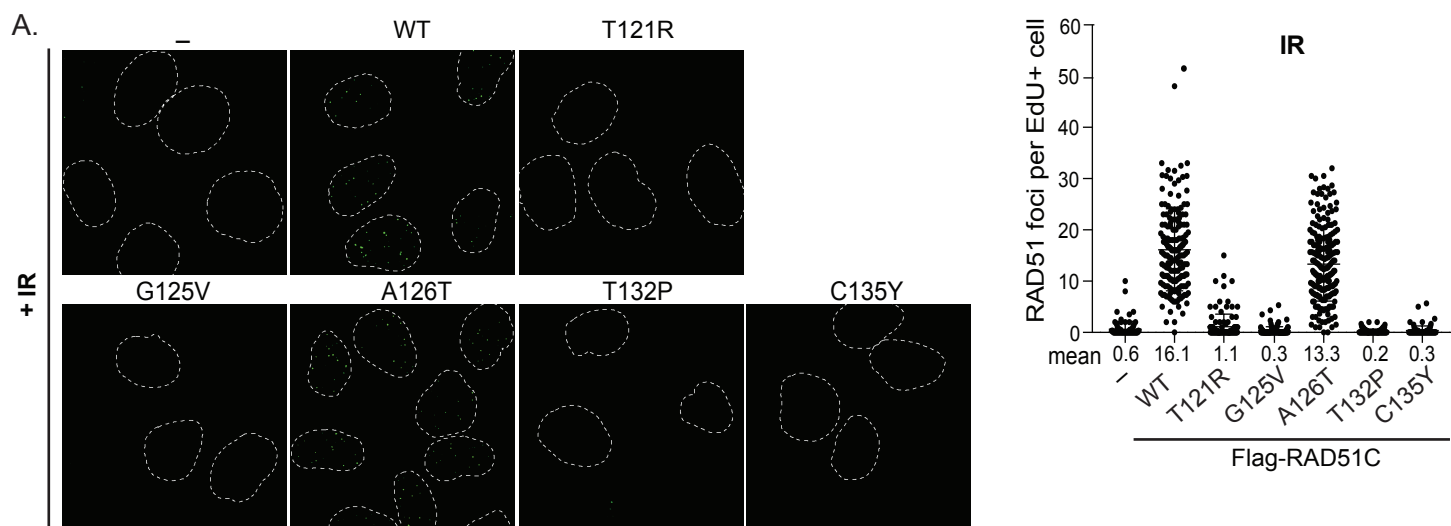
F. ATP hydrolysis was assessed by incubating BCDX2 complexes with ATP over time by thin layer chromatography, as shown in **Fig. 4D**. The table provides values calculated as pmole ATP hydrolysed pmole⁻¹ BCDX2 min⁻¹ with and without ssDNA. The graph shows results from three independent experiments performed in the absence of ssDNA.

G. The BCDX2 complex did not bind RAD51 either in the presence of ATP and MgCl₂ or in the presence of the nonhydrolyzable AMP-PNP and MgCl₂. Asterisks indicate heavy and light chains.

H. Wild-type RAD51C was able to form a stable complex with XRCC3 (CX3) while RAD51C mutants were not. CX3 complexes were affinity purified with the Flag (XRCC3-Flag) and MBP (RAD51C-MBP) tags in the presence of ATP and MgCl₂. C_{mut}X3 complexes eluted from the Flag beads nearly as efficiently as the C_{WT}X3 complex. However, when fractionated on a Superdex 200 column, they no longer formed a stable complex and were instead primarily in the void volume as protein aggregates. Protein markers: Bd, BlueDextran; Tg, thyroglobulin; Fe, ferritin; Al, aldolase; Ov, ovalbumin.

I. To determine whether the MBP tag interfered with CX3 stability, another CX3 purification scheme was devised in which the MBP tag was cleaved from RAD51C using TEV protease after the Flag affinity step (left gel). C_{WT}X3 and C_{T132P}X3 complexes were then loaded onto a Superdex 200 column (right gel). While the wild-type RAD51C elutes primarily in a complex with XRCC3-Flag, the T132P mutant elutes primarily in the void volume, as does XRCC3-Flag, suggesting aggregate formation.

Supplementary Figure S6



Supplementary Figure S6. RAD51C variants in the Walker A region exhibit defects in RAD51 focus formation and are sensitive to cisplatin and olaparib.

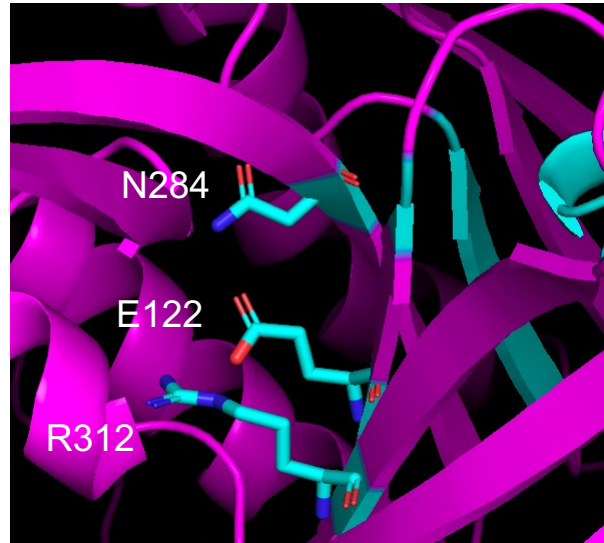
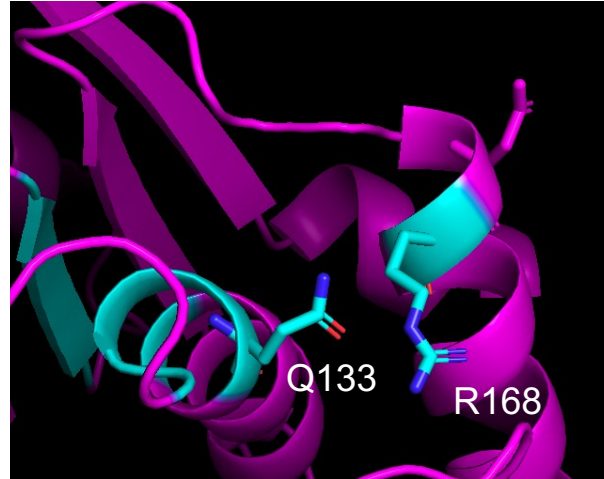
A,B. RAD51 focus formation is impaired in RAD51C mutant U2OS cells expressing HR-deficient variants treated with 4 Gy ionizing radiation with 4 hrs recovery (**A**) or 3.3 μm cisplatin for 6 hrs with 4 hrs recovery (**B**). Only S phase cells that are EdU+ were analyzed.

C,D. HR-deficient variants have impaired clonogenic survival following treatment with olaparib (**C**) or cisplatin (**D**). Cells were exposed to olaparib continuously or cisplatin for one cell cycle at the concentrations indicated and then grown for 12 days before fixation. Experiments were performed in biological triplicate and representative plate images are shown.

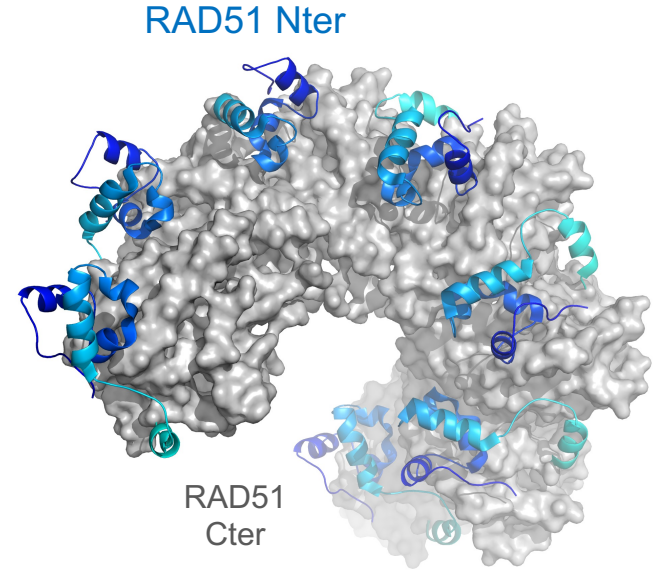
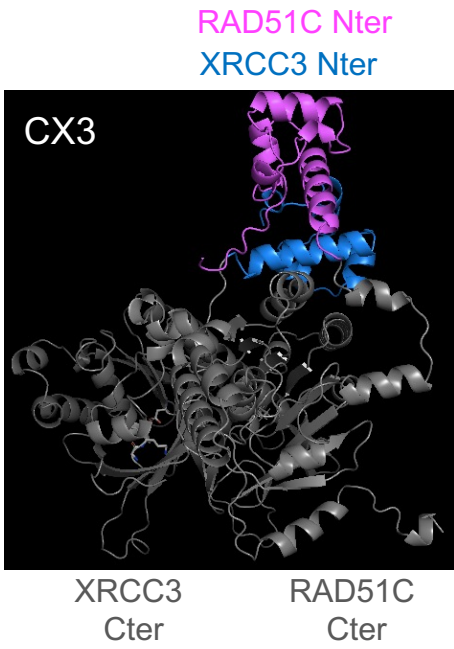
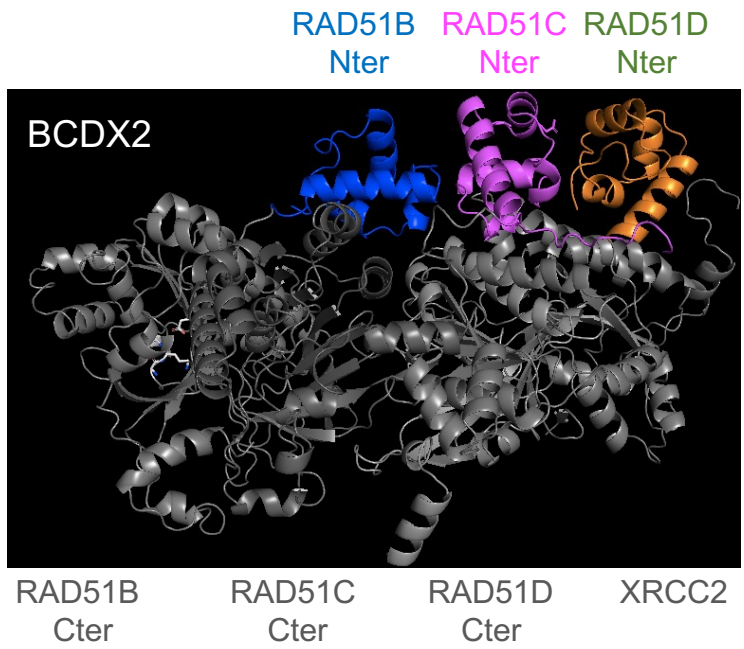
Supplementary Figure S7

A.

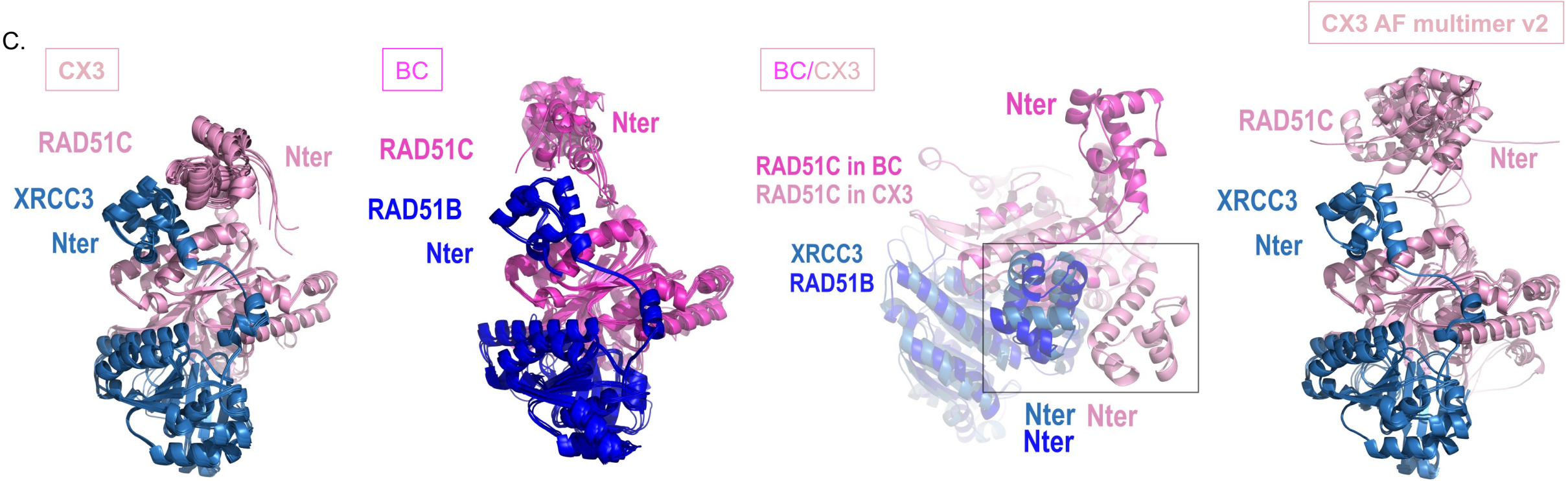
RAD51	MAMQMQLLEANADTSVEEESFGPQPI SRLEQCGI ----NANDVKKLEEAGFHTVEAVAYAP	56
RAD51B	-----MGSKK----LKRVLG----SQELCDRLSRHQILTCQDFLCLS	34
RAD51C	-----MRGKTRFRFEMQRDLVSFPL----SPAVRVKLVSAAGFQTAEEELLEVK	42
RAD51D	-----MGVLRVGLCPGLTEEMIQLLRSHRIKTVVDLVSAD	35
XRCC2	-----	0
XRCC3	-----MDLDDL----NPRIIAAIKKAKLKSVEVLHFS	31
RAD51	KKELINIKGISEAKADKILAEAAKLVPMGFTTATEFHQ---R-----RS---EIIQIT	103
RAD51B	PLELMKVITGLSYRGVHELLCMVSRACA-PMQTAYGIKA---Q-----RSADFSPAFLS	84
RAD51C	PSELSKEVGI SKAEALLETQII RRECL-TNKPRYAGTSESHKCTALELLEQEHTQGFII	101
RAD51D	LEEVAQKCGLSYKALVALRRVLLAQFS-----AFPVNG-----ADLYEELKTSTAILS	83
XRCC2	-----MCS-----AFHRAE-----SGTELLARL	18
XRCC3	GPLDKRLTNLSSPEVWHLLRTASLHLRGSSILTALQLHQOKER-----FPTQHQRLS	83
	E124/ Walker Q135/ E122 A Q133	
RAD51	TGSKELDKL-----LQGGIETGSIYEFGEFRTGKQIICHTLAVTCQLPIDRGGGEGKA	157
RAD51B	TTLSALDEA-----LHGGVACGSLTITGPPGCGKQFCIMMSILATLPTNMGGLGAV	138
RAD51C	TFCALDDI-----LGGGVPLMKTTEICGAPGVGKQLCMQLAVDVQIPECPGGVAGEA	155
RAD51D	TGIGSLDKL-----LDAGLYTGEVTEIVGGPGSGKQVCLCMAANV-----AHGLQQNV	132
XRCC2	EGRSSLEIEPNLFADEDSFVHGDIIEFHGPEGTGKTEMLYHLTARCILPKSEGGLEVEV	78
XRCC3	LGCPVLDAL-----LRGGLPLDGIIELAGRSSAGKQLALQLCLAVQFPRQHGGEAGA	137
	*. R170/ R168 * * * * * .	
RAD51	MYIDTEGTFRPEELLAVAERYGLSGSDVLDNVAYARAFNTDHQ-----	200
RAD51B	VYIDTESAFSAELVIEIAESR-----FPRYFNTEEKLLITS--SKVHLYRELT	184
RAD51C	VFIDTEGSMFVDELVDLATAACIQHLQLIAEKHKGEEHRKALEDFTLDNILSHIYFRCRD	215
RAD51D	LYVDSNGGLTASRLQLLQAKTQDEEQAEALRRI-----QVVHAFDIFQ	177
XRCC2	LFIDTDYHFDMLRLVTILEHRLSQSSEEI I KY-----CLGRFFLVYCSS	122
XRCC3	VYICTEDAFPHKRLQLMAQQPRLRTDVPGELL-----QK---LRFSGQIFIEHVAD	186
	Walker B R241/ R258	
RAD51	----TQLLYQ--ASAM-MVESRYALLIVDSATALYRTDYS--GRGELSAEIMHLARFLRM	251
RAD51B	CDEVLQRIES--LEEE-IISKGIKLVILDVSVASVVRKEFDAQLQGNLKERKPLAREASS	241
RAD51C	YTELLAQVYL--LPDFLSEHSKVLVIVDGIAPFRHDLD-----DLSIRRLNLGLAQQ	268
RAD51D	MLDVLQELRGTVAAQVVTGSSGTVIVVVVDVSVTAVVSPLLGGQQREG---LALMMQLARE	233
XRCC2	STHLLLTLYS--LESMFCSHPSLCLLILDLSAFYWI DRVNGG-ESVNLQESTLRKCSQC	179
XRCC3	VDTLLECCVNK--KVPVLLSRGMARLVVIDSVAAPFRCEPDSQAS--APRARHLQSLGAT	241
	N267/ N284	
RAD51	LLRLADEFGVAVVITNDVVAQVDGAAMFAADPKKPIG-----GNIIA	293
RAD51B	LKYLAEEFSPVILNNOITHLGALASQADLVSPADDLSLSEGTSGSSCVIAALGNTWS	301
RAD51C	MISLANNHRLAVILNDMTTKIDRNOA-----LLVLPALGESWG	306
RAD51D	LKTLARDLGMVVVITNITRDRDS-----GRCLKPALGRSWS	269
XRCC2	LEKLVNDYRLVLPATTQTIMQKASSS--EPPSHASR-----RLCDVDIDYRPVLCRAWQ	232
XRCC3	LRELSSAFQSPVLCINQVTEAMEEQGAH---GPLGF-----WDERVSPALGITWA	289
	* R299/ R312	
RAD51	HASTTILYLRKGRGET-----RICKIYDSPCLPEAE-AMFAINADGVGDAKD-----	339
RAD51B	HSVNTLILQYLDSE-----RQILIAKSPLAPFTS-FVYTIKEEGLVLQETTFCSVT	353
RAD51C	HAATIRLIFHWDR-KQ-----RLATLYKSPSQEECT-VLFQIKPQGFPRDTVVTSA CSL	357
RAD51D	FVPSTRILLDTIEGAGASGG--RRMACLAKSSRQPTGFQEMVDIGTWGTSEQSA----TL	323
XRCC2	QLVKHRRMFFSKQDDSQSSNQFSLVS-RCLKSNSLKK--HFFIIGESGVFC-----	280
XRCC3	NQLLVRLADRLREBEAALGCPARTLRVLSAPHLPPSS-CSYTI SAEGVRGTPGTQSH--	346
	*. .: * *	
RAD51	-----	339
RAD51B	QAEINWAP EILPPQPPEQLGLQ MCHHTQLIF	384
RAD51C	QTEGSLSTRKRSRDP E EEL-----	376
RAD51D	QGDQT-----	328
XRCC2	-----	280
XRCC3	-----	346



B.



C.



Supplementary Figure S7. Conservation among RAD51 paralogs.

A. Human RAD51 paralogs were aligned with RAD51 using the ClustalW program. The alignment shows that RAD51 paralogs are conserved with each other and with RAD51 at the Walker A and B motifs. In addition, a few other residues in RAD51 paralogs show conservation with RAD51, including those shown on the right.

Top right: In RAD51, the glutamine following the Walker A motif forms a salt bridge with an arginine in a neighboring alpha helix. These residues are conserved in RAD51C (RAD51, Q135:R170; RAD51C, Q133:R168) and can be similarly modeled in the RAD51C AlphaFold structure, as shown. The RAD51C Q133A mutation leads to highly defective HR.

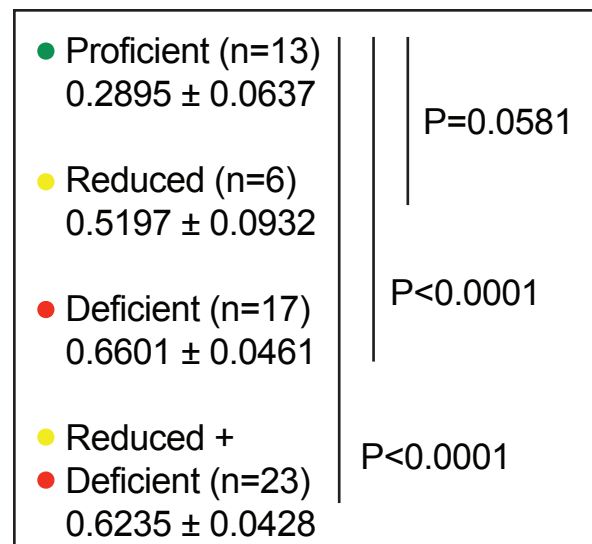
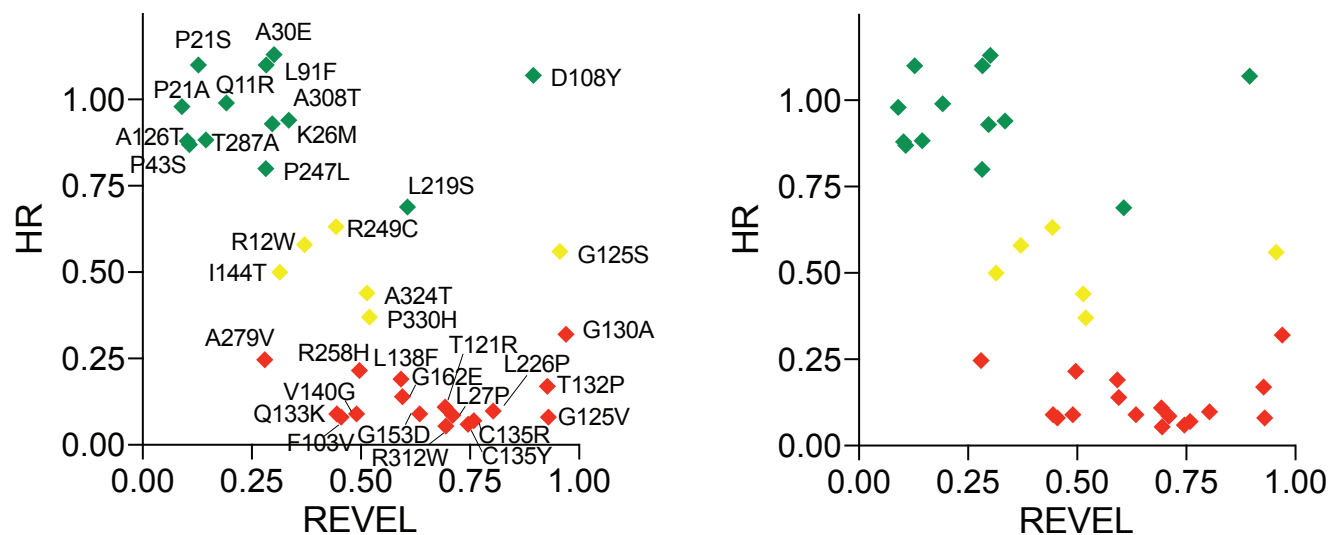
Bottom right: In RAD51, the glutamate preceding the Walker A motif forms salt bridges with an arginine and an asparagine in adjacent beta strands. These residues are conserved in RAD51C (RAD51, N267:E124:R299; RAD51C, N284:E122:R312) and can be similarly modeled in RAD51C, as shown. The RAD51C R312W mutation leads to highly defective HR.

B. The N-terminal domains (Nter) of the RAD51 paralogs interact with each other in the BCDX2 and CX3 complexes in structural models predicted by AlphaFold2 (version 1), unlike the N-termini of RAD51 in the filament (PDB: 5NWL (22)). The N-termini of the RAD51 paralogs and RAD51 are represented in the indicated colors with the rest of each protein in gray.

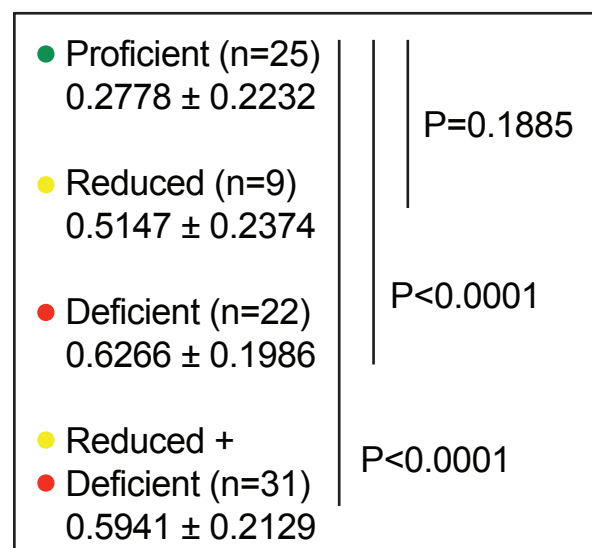
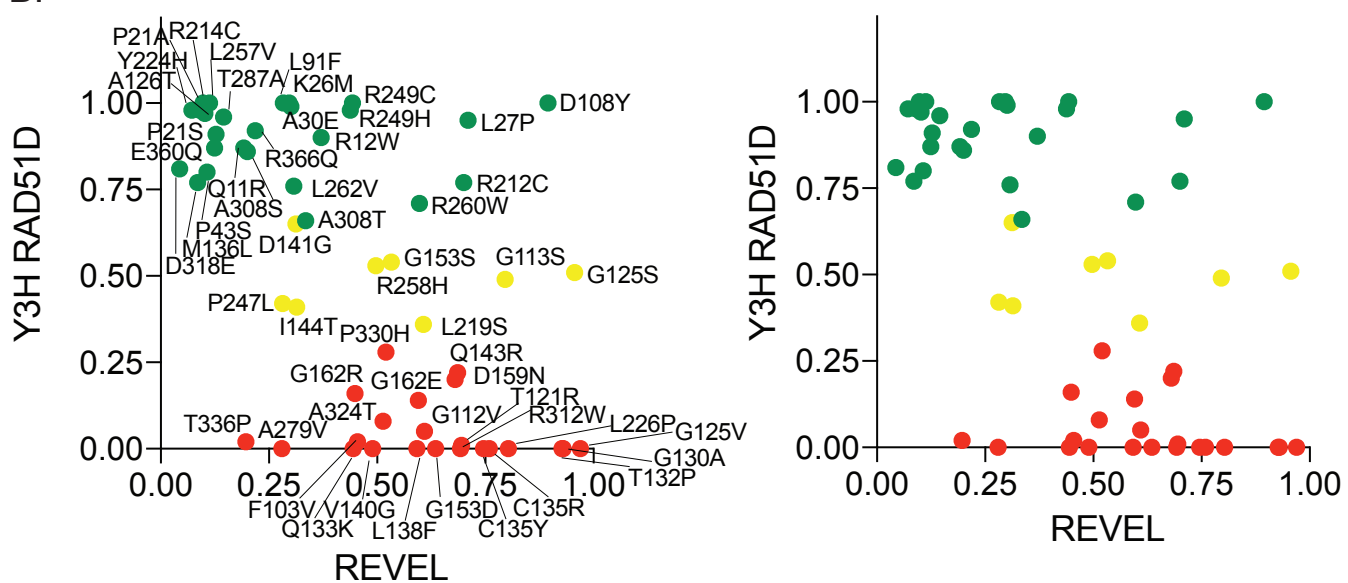
C. Structural models of the CX3 complex and the BC subcomplex predicted as a simple dimer. The superimposition of five models generated for CX3 by AlphaFold2 version 1 highlights the robustness of the predictions converging toward a compact state for the N-terminal domain of RAD51C bound to the XRCC3 N-terminal domain. The RAD51C N-terminal domain shows a different interaction with RAD51B N-terminal domain in the BC subcomplex. A superimposition of the two models is presented with a top view highlighting the drastic conformational difference for the RAD51C N-terminal domain in CX3 and BC. The position of the N-terminal domains in CX3 may limit alternative conformations with proteins such as RAD51D, disfavoring the formation of a DCX3 trimeric assembly. When we challenged AlphaFold2 to form the trimeric complex, however, it could be reliably modeled, with the orientation of the RAD51C terminal domain switching from a CX3-like conformation to a BCDX2-like one, indicating a limitation of AlphaFold2 version 1 in this context. We also re-modeled CX3 using AlphaFold2 version 2 and found that the predictions for the RAD51C N-terminal domain in CX3 are more variable than with version 1, as seen in the superimposition of the top five predicted models.

Supplementary Figure S8

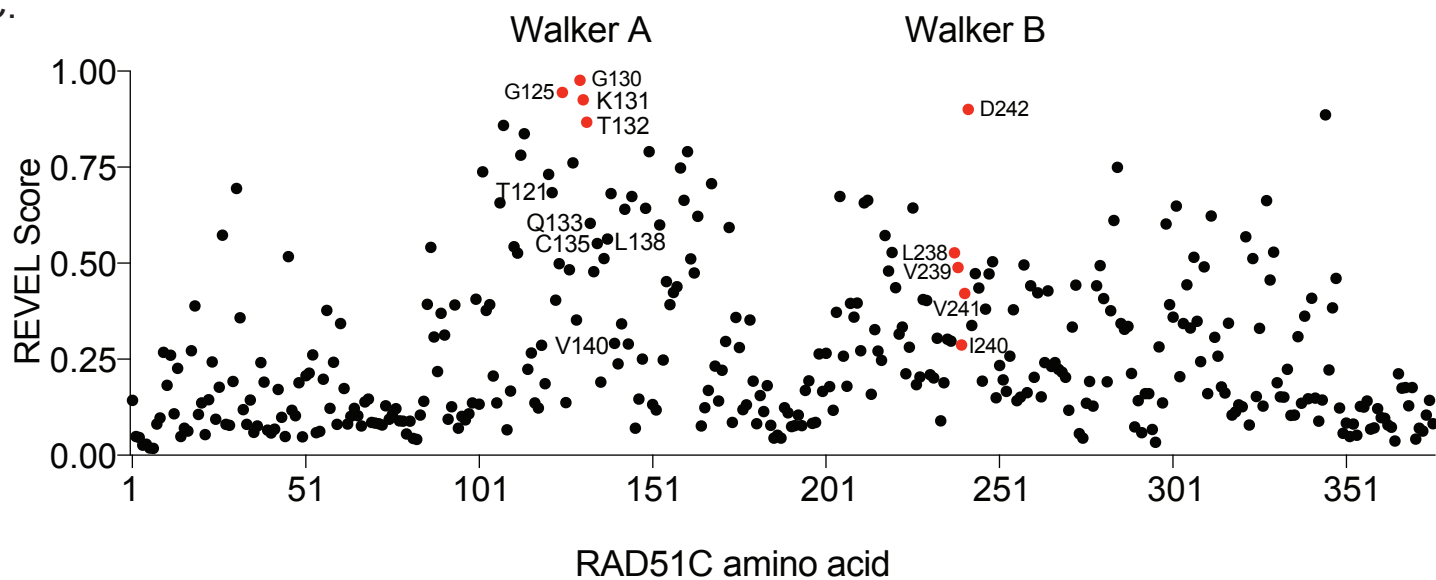
A.



B.



C.



Supplementary Figure S8. REVEL (Rare Exome Variant Ensemble Learner) scoring for the RAD51C variants analyzed in this study.

A,B. For each RAD51C variant, HR activity (**A**) and RAD51D interaction in Y3H studies (**B**) are plotted relative to the REVEL score (<https://sites.google.com/site/revelgenomics/about?authuser=0>). Plots are shown with and without variant labels. Colors indicate proficient (green), reduced (yellow), deficient (red) activity (see **Fig. 2**). Statistics shown are from an unpaired t test. Variants that were HR or interaction proficient had statistically significant lower REVEL scores on average than those that were deficient ($P < 0.0001$). Several variants proficient in functional assays but were nonetheless predicted to be deleterious by in silico tools (**Fig. 3**) had low REVEL scores, indicating better performance. Notable among these is the population variant T287A, for which homozygous individuals have been identified, and a group of variants in the N terminus (P21S, K26M, A30E, L91F).

C. Compiled REVEL scores are plotted each RAD51C residue. Each dot represents the average of the REVEL scores for all of the reported variants at that residue (**Supplementary Table S6B**). The Walker A motif GxxxxGKT residues form a cluster with the highest REVEL scores, in agreement with the strong defects observed in functional assays. The last residue of the Walker B motif (LVIVD) also scores very high. The scores for the other Walker B residues are lower in part due to frequent conservative missense substitutions among the variants (i.e., L, V, and I); nonconservative substitutions lead to higher scores (i.e., by ~ 0.1). N terminal residues tend to have low scores, in agreement with HR proficiency observed in functional assays.

Supplementary References

1. Adzhubei IA, Schmidt S, Peshkin L, Ramensky VE, Gerasimova A, Bork P, Kondrashov AS, & Sunyaev SR (2010) A method and server for predicting damaging missense mutations. *Nat. Methods* 7:248-249.
2. Sim NL, Kumar P, Hu J, Henikoff S, Schneider G, & Ng PC (2012) SIFT web server: predicting effects of amino acid substitutions on proteins. *Nucleic Acids Res.* 40:W452-457.
3. Choi Y & Chan AP (2015) PROVEAN web server: a tool to predict the functional effect of amino acid substitutions and indels. *Bioinformatics* 31:2745-2747.
4. Choi Y, Sims GE, Murphy S, Miller JR, & Chan AP (2012) Predicting the functional effect of amino acid substitutions and indels. *PLoS One* 7:e46688.
5. Garcin EB, Gon S, Sullivan MR, Brunette GJ, Cian A, Concordet JP, Giovannangeli C, Dirks WG, *et al.* (2019) Differential Requirements for the RAD51 Paralogs in Genome Repair and Maintenance in Human Cells. *PLoS Genet.* 15:e1008355.
6. Feng W & Jasin M (2017) BRCA2 suppresses replication stress-induced mitotic and G1 abnormalities through homologous recombination. *Nat Commun.* 8:525.
7. Brunet E, Simsek D, Tomishima M, DeKolver R, Choi VM, Gregory P, Urnov F, Weinstock DM, *et al.* (2009) Chromosomal translocations induced at specified loci in human stem cells. *Proc. Natl. Acad. Sci. U S A* 106:10620-10625.
8. Richardson C, Moynahan ME, & Jasin M (1998) Double-strand break repair by interchromosomal recombination: suppression of chromosomal translocations. *Genes Dev.* 12:3831-3842.
9. McClendon TB, Sullivan MR, Bernstein KA, & Yanowitz JL (2016) Promotion of Homologous Recombination by SWS-1 in Complex with RAD-51 Paralogs in *Caenorhabditis elegans*. *Genetics* 203:133-145.
10. Knop M, Siegers K, Pereira G, Zachariae W, Winsor B, Nasmyth K, & Schiebel E (1999) Epitope tagging of yeast genes using a PCR-based strategy: more tags and improved practical routines. *Yeast* 15:963-972.
11. Gaines WA, Godin SK, Kabbinavar FF, Rao T, VanDemark AP, Sung P, & Bernstein KA (2015) Promotion of presynaptic filament assembly by the ensemble of *S. cerevisiae* Rad51 paralogues with Rad52. *Nat. Commun.* 6:7834.
12. UniProt C (2021) UniProt: the universal protein knowledgebase in 2021. *Nucleic Acids Res.* 49:D480-D489.
13. Steinegger M & Soding J (2017) MMseqs2 enables sensitive protein sequence searching for the analysis of massive data sets. *Nat. Biotechnol.* 35:1026-1028.
14. Mirdita M, Schütze K, Moriwaki Y, Heo L, Ovchinnikov S, & Steinegger M (2021) ColabFold - Making protein folding accessible to all. *bioRxiv:2021.2008.2015.456425*.
15. Katoh K & Standley DM (2013) MAFFT multiple sequence alignment software version 7: improvements in performance and usability. *Mol. Biol. Evol.* 30:772-780.
16. Jumper J, Evans R, Pritzel A, Green T, Figurnov M, Ronneberger O, Tunyasuvunakool K, Bates R, *et al.* (2021) Highly accurate protein structure prediction with AlphaFold. *Nature* 596:583-589.
17. Evans R, O'Neill M, Pritzel A, Antropova N, Senior A, Green T, Židek A, Bates R, *et al.* (2021) Protein complex prediction with AlphaFold-Multimer. *bioRxiv:2021.2010.2004.463034*.
18. Leman JK, Weitzner BD, Lewis SM, Adolf-Bryfogle J, Alam N, Alford RF, Aprahamian M, Baker D, *et al.* (2020) Macromolecular modeling and design in Rosetta: recent methods and frameworks. *Nat Methods* 17:665-680.
19. Hubbard SJ & Thornton JM (1993) 'NACCESS'. *Computer Program, Department of Biochemistry and Molecular Biology, University College London*.
20. Schild D, Lio YC, Collins DW, Tsomondo T, & Chen DJ (2000) Evidence for simultaneous protein interactions between human Rad51 paralogs. *J Biol Chem* 275:16443-16449.
21. Baldock RA, Pressimone CA, Baird JM, Khodakov A, Luong TT, McKenzie KG, Smith CM, Karpenshif Y, *et al.* (2019) RAD51D splice variants and cancer-associated mutations reveal XRCC2 interaction to be critical for homologous recombination. *DNA Repair* 76:99-107.
22. Brouwer I, Moschetti T, Candelli A, Garcin EB, Modesti M, Pellegrini L, Wuite GJ, & Peterman EJ (2018) Two distinct conformational states define the interaction of human RAD51-ATP with single-stranded DNA. *EMBO J.* 37.
23. Xu J, Zhao L, Xu Y, Zhao W, Sung P, & Wang HW (2017) Cryo-EM structures of human RAD51 recombinase filaments during catalysis of DNA-strand exchange. *Nat. Struct. Mol. Biol.* 24:40-46.

Supplementary Table S1. RAD51C missense variants reported in ClinVar.

Variant	Clinical Significance (Last Reviewed)	
M1L	Uncertain significance(Last reviewed: Sep 8, 2020)	
M1V	Uncertain significance(Last reviewed: Dec 3, 2020)	
M1I	Uncertain significance(Last reviewed: Dec 15, 2020)	
R2G	Uncertain significance(Last reviewed: Dec 20, 2018)	
G3W	Uncertain significance(Last reviewed: Oct 25, 2019)	
G3R	Conflicting interpretations of pathogenicity(Last reviewed: Jan 20, 2021)	
G3E	Uncertain significance(Last reviewed: Sep 20, 2018)	
G3A	Uncertain significance(Last reviewed: Jan 13, 2017)	
T5R	Uncertain significance(Last reviewed: Jul 25, 2019)	
T5M	Uncertain significance(Last reviewed: Oct 29, 2020)	
F6V	Uncertain significance(Last reviewed: May 28, 2019)	
F6Y	Uncertain significance(Last reviewed: Oct 31, 2019)	
F6L	Uncertain significance(Last reviewed: Dec 30, 2019)	
R7G	Uncertain significance(Last reviewed: Nov 4, 2018)	
R7S	Uncertain significance(Last reviewed: Oct 28, 2020)	
R7C	Uncertain significance(Last reviewed: Jun 21, 2020)	
R7L	Uncertain significance(Last reviewed: Aug 6, 2020)	
R7P	Uncertain significance(Last reviewed: May 1, 2019)	
R7H	Uncertain significance(Last reviewed: Mar 30, 2018)	
F8L	Uncertain significance(Last reviewed: Aug 20, 2020)	
E9Q	Uncertain significance(Last reviewed: Nov 18, 2018)	
E9V	Uncertain significance(Last reviewed: Oct 7, 2020)	
M10L	Uncertain significance(Last reviewed: Dec 22, 2020)	
M10T	Uncertain significance(Last reviewed: Apr 28, 2020)	
M10R	Uncertain significance(Last reviewed: Oct 28, 2020)	
M10I	Uncertain significance(Last reviewed: Dec 18, 2019)	
Q11R	Uncertain significance(Last reviewed: Sep 8, 2020)	
R12G	Uncertain significance(Last reviewed: Aug 25, 2018)	
R12W	Uncertain significance(Last reviewed: Jun 10, 2021)	
R12P	Uncertain significance(Last reviewed: Aug 13, 2019)	
R12Q	Uncertain significance(Last reviewed: Mar 29, 2019)	
D13N	Uncertain significance(Last reviewed: Apr 13, 2018)	
D13H	Uncertain significance(Last reviewed: Mar 30, 2018)	
V15A	Uncertain significance(Last reviewed: Aug 4, 2020)	
V15G	Uncertain significance(Last reviewed: Feb 26, 2020)	

S16G	Uncertain significance(Last reviewed: Mar 5, 2020)	
S16N	Uncertain significance(Last reviewed: Dec 29, 2017)	
F17C	Uncertain significance(Last reviewed: Sep 2, 2020)	
F17S	Uncertain significance(Last reviewed: Jul 25, 2020)	
F17L	Uncertain significance(Last reviewed: Feb 16, 2019)	
P18S	Uncertain significance(Last reviewed: Sep 9, 2020)	
P18R	Uncertain significance(Last reviewed: Sep 4, 2019)	
P18L	Uncertain significance(Last reviewed: Aug 3, 2020)	
L19M	Uncertain significance(Last reviewed: Jan 2, 2017)	
L19P	Uncertain significance(Last reviewed: Jan 8, 2020)	
S20F	Uncertain significance(Last reviewed: Sep 14, 2019)	
S20C	Uncertain significance(Last reviewed: Mar 30, 2018)	
P21A	Uncertain significance(Last reviewed: Mar 29, 2019)	
P21S	Uncertain significance(Last reviewed: Mar 27, 2019)	
P21L	Uncertain significance(Last reviewed: Aug 10, 2020)	
V23G	Uncertain significance(Last reviewed: May 1, 2019)	
R24G	Uncertain significance(Last reviewed: Jan 3, 2019)	
R24W	Uncertain significance(Last reviewed: Nov 13, 2015)	
R24L	Uncertain significance(Last reviewed: Aug 11, 2016)	
R24Q	Uncertain significance(Last reviewed: Jul 21, 2019)	
V25L	Uncertain significance(Last reviewed: Dec 13, 2019)	
V25M	Uncertain significance(Last reviewed: Oct 26, 2018)	
V25A	Uncertain significance(Last reviewed: Jan 20, 2020)	
K26E	Uncertain significance(Last reviewed: Sep 28, 2019)	
K26M	Uncertain significance(Last reviewed: Oct 7, 2020)	
L27P	Uncertain significance(Last reviewed: May 11, 2021)	
V28L	Uncertain significance(Last reviewed: May 9, 2016)	
V28M	Uncertain significance(Last reviewed: Jun 20, 2016)	
S29F	Uncertain significance(Last reviewed: Jan 23, 2020)	
A30P	Uncertain significance(Last reviewed: Oct 5, 2020)	
A30S	Uncertain significance(Last reviewed: Apr 3, 2019)	
A30V	Uncertain significance(Last reviewed: Oct 9, 2020)	
G31E	Uncertain significance(Last reviewed: Sep 12, 2019)	
F32L	Uncertain significance(Last reviewed: Oct 22, 2018)	
Q33H	Uncertain significance(Last reviewed: Aug 8, 2019)	
T34I	Uncertain significance(Last reviewed: Jul 26, 2019)	
A35S	Uncertain significance(Last reviewed: Jun 17, 2020)	
A35V	Uncertain significance(Last reviewed: Dec 23, 2019)	

A35G	Uncertain significance(Last reviewed: Oct 21, 2020)	
E36K	Conflicting interpretations of pathogenicity(Last reviewed: Oct 3, 2020)	
E37Q	Uncertain significance(Last reviewed: Sep 4, 2020)	
L38P	Uncertain significance(Last reviewed: Apr 25, 2019)	
L39I	Uncertain significance(Last reviewed: Oct 16, 2020)	
L39V	Uncertain significance(Last reviewed: Oct 1, 2020)	
E40K	Uncertain significance(Last reviewed: Feb 10, 2020)	
E40G	Uncertain significance(Last reviewed: Oct 2, 2017)	
V41L	Uncertain significance(Last reviewed: Jul 5, 2018)	
V41M	Uncertain significance(Last reviewed: Mar 12, 2021)	
V41L	Uncertain significance(Last reviewed: May 29, 2020)	
P43T	Uncertain significance(Last reviewed: Nov 17, 2018)	
P43S	Uncertain significance(Last reviewed: Feb 28, 2019)	
P43L	Uncertain significance(Last reviewed: Oct 3, 2019)	
E45K	Uncertain significance(Last reviewed: Jan 9, 2018)	
E45A	Uncertain significance(Last reviewed: Aug 24, 2020)	
E45G	Conflicting interpretations of pathogenicity(Last reviewed: Nov 1, 2020)	
E45D	Uncertain significance(Last reviewed: May 22, 2019)	
L46F	Uncertain significance(Last reviewed: Mar 29, 2019)	
L46I	Uncertain significance(Last reviewed: Mar 29, 2017)	
S47G	Uncertain significance(Last reviewed: Oct 8, 2019)	
S47R	Uncertain significance(Last reviewed: Dec 27, 2019)	
S47N	Uncertain significance(Last reviewed: Aug 6, 2020)	
E49K	Uncertain significance(Last reviewed: May 7, 2019)	
G51V	Uncertain significance(Last reviewed: Feb 24, 2020)	
G51A	Uncertain significance(Last reviewed: Jul 21, 2019)	
I52V	Uncertain significance(Last reviewed: Dec 31, 2017)	
I52L	Uncertain significance(Last reviewed: Oct 19, 2020)	
I52M	Uncertain significance(Last reviewed: Aug 8, 2019)	
S53P	Uncertain significance(Last reviewed: Dec 6, 2019)	
S53C	Uncertain significance(Last reviewed: Jan 31, 2020)	
K54E	Uncertain significance(Last reviewed: Apr 24, 2018)	
K54T	Uncertain significance(Last reviewed: Jun 21, 2020)	
A55T	Uncertain significance(Last reviewed: Oct 21, 2020)	
A55V	Uncertain significance(Last reviewed: Sep 23, 2020)	
E56G	Uncertain significance(Last reviewed: Dec 26, 2019)	
A57T	Uncertain significance(Last reviewed: Jul 21, 2020)	
A57G	Uncertain significance(Last reviewed: Mar 10, 2020)	

T60A	Uncertain significance(Last reviewed: Jul 1, 2020)	
Q62R	Uncertain significance(Last reviewed: Sep 2, 2020)	
Q62H	Uncertain significance(Last reviewed: Nov 4, 2019)	
I63M	Uncertain significance(Last reviewed: Jan 16, 2020)	
I64V	Uncertain significance(Last reviewed: Oct 25, 2020)	
I64F	Uncertain significance(Last reviewed: Jun 29, 2020)	
I64T	Uncertain significance(Last reviewed: Aug 10, 2017)	
R65G	Uncertain significance(Last reviewed: Oct 24, 2016)	
R65T	Uncertain significance(Last reviewed: Jan 27, 2021)	
R66S	Uncertain significance(Last reviewed: Dec 21, 2016)	
E67Q	Uncertain significance(Last reviewed: Oct 18, 2019)	
E67G	Uncertain significance(Last reviewed: Nov 16, 2020)	
L69P	Uncertain significance(Last reviewed: Jul 21, 2019)	
T70I	Uncertain significance(Last reviewed: Dec 6, 2016)	
N71Y	Uncertain significance(Last reviewed: Mar 8, 2020)	
N71S	Uncertain significance(Last reviewed: Oct 29, 2020)	
N71T	Uncertain significance(Last reviewed: Aug 1, 2019)	
K72E	Uncertain significance(Last reviewed: Jan 20, 2021)	
P73S	Uncertain significance(Last reviewed: Feb 2, 2020)	
P73A	Uncertain significance(Last reviewed: Jun 21, 2017)	
Y75C	Uncertain significance(Last reviewed: Jul 22, 2020)	
A76T	Uncertain significance(Last reviewed: Oct 2, 2019)	
A76P	Uncertain significance(Last reviewed: Oct 28, 2019)	
A76G	Uncertain significance(Last reviewed: Nov 8, 2019)	
A76V	Uncertain significance(Last reviewed: Feb 28, 2019)	
G77D	Uncertain significance(Last reviewed: Sep 16, 2020)	
G77A	Uncertain significance(Last reviewed: Feb 7, 2019)	
T78I	Uncertain significance(Last reviewed: Oct 27, 2020)	
S79P	Uncertain significance(Last reviewed: May 15, 2018)	
S79T	Uncertain significance(Last reviewed: Apr 3, 2019)	
S79F	Uncertain significance(Last reviewed: Sep 15, 2020)	
E80G	Uncertain significance(Last reviewed: Jun 6, 2019)	
E80D	Uncertain significance(Last reviewed: Mar 29, 2018)	
S81L	Uncertain significance(Last reviewed: Dec 18, 2019)	
H82Y	Uncertain significance(Last reviewed: Nov 29, 2018)	
H82R	Uncertain significance(Last reviewed: Jul 26, 2020)	
H82Q	Uncertain significance(Last reviewed: Sep 21, 2017)	
K83E	Uncertain significance(Last reviewed: Jun 3, 2020)	

K83T	Uncertain significance(Last reviewed: Jun 15, 2020)	
K83R	Uncertain significance(Last reviewed: Jun 22, 2017)	
K84N	Uncertain significance(Last reviewed: Oct 20, 2020)	
C85R	Uncertain significance(Last reviewed: Dec 6, 2017)	
C85G	Uncertain significance(Last reviewed: Aug 14, 2020)	
C85Y	Uncertain significance(Last reviewed: Jun 23, 2020)	
T86I	Uncertain significance(Last reviewed: Mar 18, 2020)	
A87S	Uncertain significance(Last reviewed: Mar 29, 2019)	
A87T	Uncertain significance(Last reviewed: May 20, 2020)	
A87E	Uncertain significance(Last reviewed: Mar 29, 2019)	
L88V	Uncertain significance(Last reviewed: Jan 5, 2018)	
E89Q	Uncertain significance(Last reviewed: Oct 14, 2019)	
E89K	Uncertain significance(Last reviewed: Jun 21, 2020)	
E89G	Uncertain significance(Last reviewed: Sep 15, 2020)	
L90F	Uncertain significance(Last reviewed: Jan 16, 2020)	
L90R	Uncertain significance(Last reviewed: May 4, 2020)	
L90H	Uncertain significance(Last reviewed: Jul 21, 2015)	
L91F	Uncertain significance(Last reviewed: Feb 10, 2017)	
L91P	Uncertain significance(Last reviewed: Sep 14, 2017)	
E92K	Uncertain significance(Last reviewed: Nov 14, 2019)	
E94K	Uncertain significance(Last reviewed: Nov 20, 2019)	
H95Y	Uncertain significance(Last reviewed: Dec 27, 2019)	
H95L	Uncertain significance(Last reviewed: Feb 20, 2019)	
H95P	Uncertain significance(Last reviewed: May 30, 2019)	
H95Q	Uncertain significance(Last reviewed: Oct 7, 2020)	
T96P	Uncertain significance(Last reviewed: Jul 19, 2019)	
T96S	Uncertain significance(Last reviewed: Jan 14, 2020)	
Q97E	Uncertain significance(Last reviewed: Sep 23, 2020)	
Q97R	Uncertain significance(Last reviewed: Oct 26, 2019)	
G98V	Uncertain significance(Last reviewed: Sep 27, 2019)	
G98A	Uncertain significance(Last reviewed: May 16, 2019)	
F99L	Uncertain significance(Last reviewed: Aug 16, 2016)	
F99S	Uncertain significance(Last reviewed: Oct 7, 2020)	
I100K	Uncertain significance(Last reviewed: May 18, 2019)	
I101V	Uncertain significance(Last reviewed: May 18, 2021)	
T102A	Uncertain significance(Last reviewed: Jun 6, 2020)	
T102N	Uncertain significance(Last reviewed: Nov 4, 2019)	
T102I	Uncertain significance(Last reviewed: Nov 4, 2019)	

F103I	Uncertain significance(Last reviewed: May 14, 2018)	
F103V	Uncertain significance(Last reviewed: Jun 13, 2017)	
F103L	Uncertain significance(Last reviewed: Apr 24, 2019)	
C104Y	Uncertain significance(Last reviewed: Dec 18, 2018)	
A106V	Uncertain significance(Last reviewed: Jun 6, 2019)	
D108H	Uncertain significance(Last reviewed: Nov 28, 2018)	
D108G	Uncertain significance(Last reviewed: Sep 18, 2020)	
D109Y	Uncertain significance(Last reviewed: Mar 29, 2019)	
I110S	Uncertain significance(Last reviewed: Jan 16, 2019)	
L111F	Uncertain significance(Last reviewed: Oct 22, 2018)	
G112E	Uncertain significance(Last reviewed: Dec 3, 2018)	
G112V	Uncertain significance(Last reviewed: Feb 15, 2021)	
G112A	Uncertain significance(Last reviewed: Oct 16, 2020)	
G113R	Uncertain significance(Last reviewed: May 29, 2020)	
G113D	Uncertain significance(Last reviewed: Oct 22, 2019)	
G114R	Uncertain significance(Last reviewed: Aug 14, 2020)	
G114V	Uncertain significance(Last reviewed: Apr 3, 2019)	
V115A	Uncertain significance(Last reviewed: Dec 29, 2018)	
P116H	Uncertain significance(Last reviewed: Oct 13, 2019)	
L117S	Uncertain significance(Last reviewed: Dec 7, 2018)	
L117F	Uncertain significance(Last reviewed: May 21, 2019)	
M118I	Uncertain significance(Last reviewed: May 24, 2019)	
K119R	Uncertain significance(Last reviewed: Nov 16, 2019)	
T121A	Uncertain significance(Last reviewed: Oct 27, 2020)	
T121I	Uncertain significance(Last reviewed: Aug 12, 2019)	
E122D	Uncertain significance(Last reviewed: Oct 6, 2020)	
I123V	Uncertain significance(Last reviewed: Jul 19, 2017)	
C124G	Uncertain significance(Last reviewed: Mar 29, 2019)	
C124S	Uncertain significance(Last reviewed: Sep 8, 2020)	
G125S	Uncertain significance(Last reviewed: Jul 31, 2020)	
G125D	Uncertain significance(Last reviewed: Mar 10, 2020)	
G125V	Pathogenic, risk factor(Last reviewed: Feb 28, 2020)	
A126T	Benign/Likely benign(Last reviewed: Dec 7, 2020)	
A126V	Uncertain significance(Last reviewed: Nov 12, 2018)	
P127S	Uncertain significance(Last reviewed: Dec 14, 2017)	
P127T	Uncertain significance(Last reviewed: Feb 29, 2020)	
G128R	Uncertain significance(Last reviewed: May 29, 2020)	
G128D	Uncertain significance(Last reviewed: Mar 29, 2019)	

G128A	Uncertain significance(Last reviewed: Nov 29, 2018)	
V129I	Uncertain significance(Last reviewed: Jan 30, 2017)	
V129A	Uncertain significance(Last reviewed: Jul 2, 2018)	
G130A	Uncertain significance(Last reviewed: Jul 15, 2019)	
K131I	Uncertain significance(Last reviewed: Jul 18, 2018)	
T132P	Likely pathogenic(Last reviewed: Jan 28, 2021)	
T132I	Uncertain significance(Last reviewed: May 22, 2015)	
T132R	Uncertain significance(Last reviewed: Feb 1, 2020)	
Q133K	Uncertain significance(Last reviewed: Oct 29, 2018)	
Q133E	Uncertain significance(Last reviewed: Sep 2, 2020)	
L134S	Uncertain significance(Last reviewed: Nov 25, 2017)	
C135R, (W135R)#	Uncertain significance(Last reviewed: Sep 9, 2020)	#Isoform 2
C135F, (W135L)#	Likely pathogenic(Last reviewed: Jun 18, 2019)	#Isoform 2
C135S, (W135S)#	Pathogenic/Likely pathogenic(Last reviewed: Mar 19, 2021)	#Isoform 2
C135Y, (W135*)#	Likely pathogenic(Last reviewed: Oct 7, 2020)	#Isoform 2
M136L	Uncertain significance(Last reviewed: Oct 15, 2020)	
M136I	Uncertain significance(Last reviewed: Oct 20, 2020)	
Q137P	Uncertain significance(Last reviewed: Apr 15, 2020)	
Q137H	Uncertain significance(Last reviewed: Sep 11, 2020)	
L138F	Pathogenic/Likely pathogenic(Last reviewed: Oct 27, 2020)	
A139T	Uncertain significance(Last reviewed: Oct 28, 2019)	
A139P	Uncertain significance(Last reviewed: May 2, 2019)	
A139V	Uncertain significance(Last reviewed: Sep 13, 2019)	
V140L	Uncertain significance(Last reviewed: Apr 7, 2017)	
V140I	Uncertain significance(Last reviewed: Aug 3, 2020)	
V140E	Uncertain significance(Last reviewed: Mar 9, 2020)	
D141N	Uncertain significance(Last reviewed: Feb 18, 2015)	
D141G	Uncertain significance(Last reviewed: Jul 27, 2020)	
D141E	Uncertain significance(Last reviewed: Nov 9, 2019)	
Q143R	Uncertain significance(Last reviewed: Oct 30, 2020)	
I144L	Uncertain significance(Last reviewed: Nov 15, 2018)	
I144T	Uncertain significance(Last reviewed: May 27, 2021)	
I144M	Uncertain significance(Last reviewed: Apr 29, 2016)	
P145T	Uncertain significance(Last reviewed: Mar 14, 2019)	
P145S	Uncertain significance(Last reviewed: Sep 26, 2018)	
P145A	Uncertain significance(Last reviewed: May 26, 2016)	
P145L	Uncertain significance(Last reviewed: May 27, 2020)	
C147R	Uncertain significance(Last reviewed: Mar 19, 2020)	

C147Y	Uncertain significance(Last reviewed: Mar 5, 2019)	
F148C	Uncertain significance(Last reviewed: May 24, 2019)	
F148S	Uncertain significance(Last reviewed: Oct 14, 2015)	
G149E	Uncertain significance(Last reviewed: Oct 23, 2019)	
G150R	Uncertain significance(Last reviewed: Nov 28, 2019)	
G150E	Uncertain significance(Last reviewed: Sep 8, 2014)	
V151L	Uncertain significance(Last reviewed: May 31, 2019)	
V151M	Uncertain significance(Last reviewed: Jan 26, 2021)	
A152T	Uncertain significance(Last reviewed: Nov 26, 2019)	
A152S	Uncertain significance(Last reviewed: Oct 4, 2020)	
G153D	Uncertain significance(Last reviewed: Jul 20, 2020)	
E154K	Uncertain significance(Last reviewed: Sep 3, 2018)	
E154G	Conflicting interpretations of pathogenicity(Last reviewed: Jun 13, 2020)	
A155T	Uncertain significance(Last reviewed: Feb 20, 2020)	
A155G	Uncertain significance(Last reviewed: May 30, 2019)	
V156D	Uncertain significance(Last reviewed: Mar 28, 2019)	
F157C	Uncertain significance(Last reviewed: Feb 21, 2017)	
I158T	Uncertain significance(Last reviewed: Feb 27, 2020)	
D159N	Conflicting interpretations of pathogenicity(Last reviewed: Nov 2, 2014)	
D159G	Uncertain significance(Last reviewed: May 15, 2018)	
D159A	Uncertain significance(Last reviewed: May 20, 2019)	
D159E	Uncertain significance(Last reviewed: Aug 21, 2020)	
E161Q	Uncertain significance(Last reviewed: Oct 30, 2019)	
E161V	Uncertain significance(Last reviewed: Apr 26, 2020)	
E161D	Uncertain significance(Last reviewed: Jan 21, 2020)	
G162E	Uncertain significance(Last reviewed: Jul 30, 2020)	
S163G	Uncertain significance(Last reviewed: Jan 26, 2020)	
S163C	Uncertain significance(Last reviewed: Aug 9, 2017)	
S163N	Uncertain significance(Last reviewed: Sep 26, 2019)	
S163R	Uncertain significance(Last reviewed: Nov 9, 2020)	
F164V	Uncertain significance(Last reviewed: Jan 6, 2017)	
F164S	Uncertain significance(Last reviewed: Sep 22, 2019)	
F164L	Uncertain significance(Last reviewed: Jan 6, 2021)	
M165V	Uncertain significance(Last reviewed: Dec 27, 2017)	
M165T	Uncertain significance(Last reviewed: Jul 20, 2020)	
M165I	Uncertain significance(Last reviewed: Nov 29, 2018)	
V166A	Uncertain significance(Last reviewed: Mar 30, 2018)	
D167H	Uncertain significance(Last reviewed: Sep 22, 2019)	

D167G	Uncertain significance(Last reviewed: Mar 18, 2020)	
D167A	Uncertain significance(Last reviewed: May 25, 2019)	
R168G	Uncertain significance(Last reviewed: Mar 5, 2019)	
V169A	Conflicting interpretations of pathogenicity(Last reviewed: Jul 1, 2021)	
V170I	Uncertain significance(Last reviewed: Jan 19, 2019)	
D171A	Uncertain significance(Last reviewed: May 18, 2015)	
D171E	Uncertain significance(Last reviewed: Oct 29, 2019)	
L172F	Uncertain significance(Last reviewed: Aug 19, 2020)	
L172V	Uncertain significance(Last reviewed: Sep 4, 2015)	
L172P	Uncertain significance(Last reviewed: Dec 8, 2020)	
T174A	Uncertain significance(Last reviewed: Aug 17, 2021)	
T174I	Uncertain significance(Last reviewed: Jan 15, 2020)	
A175S	Uncertain significance(Last reviewed: Dec 31, 2018)	
A175T	Uncertain significance(Last reviewed: Mar 5, 2021)	
C176R	Uncertain significance(Last reviewed: Oct 28, 2020)	
I177V	Uncertain significance(Last reviewed: Jun 5, 2019)	
Q178P	Uncertain significance(Last reviewed: Aug 25, 2011)	
Q178R	Uncertain significance(Last reviewed: Dec 11, 2019)	
Q178H	Uncertain significance(Last reviewed: Apr 27, 2018)	
H179R	Uncertain significance(Last reviewed: Jan 18, 2021)	
H179Q	Uncertain significance(Last reviewed: Oct 9, 2020)	
L180R	Uncertain significance(Last reviewed: Oct 3, 2019)	
Q181R	Uncertain significance(Last reviewed: Jul 4, 2019)	
L182F	Uncertain significance(Last reviewed: Apr 3, 2019)	
I183V	Uncertain significance(Last reviewed: Aug 31, 2020)	
I183T	Uncertain significance(Last reviewed: Oct 13, 2020)	
A184T	Uncertain significance(Last reviewed: Mar 18, 2020)	
E185Q	Uncertain significance(Last reviewed: May 10, 2016)	
E185G	Uncertain significance(Last reviewed: May 3, 2019)	
K186Q	Uncertain significance(Last reviewed: Jan 31, 2019)	
K186E	Uncertain significance(Last reviewed: Apr 5, 2018)	
H187Q	Uncertain significance(Last reviewed: Oct 14, 2020)	
K188M	Conflicting interpretations of pathogenicity(Last reviewed: Nov 16, 2020)	
K188N	Uncertain significance(Last reviewed: Sep 10, 2020)	
G189R	Uncertain significance(Last reviewed: Aug 27, 2019)	
G189E	Uncertain significance(Last reviewed: Dec 27, 2019)	
E190K	Uncertain significance(Last reviewed: Mar 29, 2020)	
E191K	Uncertain significance(Last reviewed: Jul 23, 2018)	

H192Y	Uncertain significance(Last reviewed: Nov 16, 2018)	
H192Q	Uncertain significance(Last reviewed: Jun 16, 2020)	
R193Q	Conflicting interpretations of pathogenicity(Last reviewed: Oct 19, 2020)	
A195T	Uncertain significance(Last reviewed: Sep 25, 2016)	
E197K	Uncertain significance(Last reviewed: Oct 17, 2018)	
D198G	Uncertain significance(Last reviewed: Jan 15, 2020)	
T200A	Uncertain significance(Last reviewed: Nov 6, 2019)	
L201V	Uncertain significance(Last reviewed: Dec 2, 2020)	
L201P	Uncertain significance(Last reviewed: Mar 29, 2019)	
D202G	Uncertain significance(Last reviewed: Nov 21, 2018)	
D202E	Uncertain significance(Last reviewed: Jun 2, 2020)	
N203D	Uncertain significance(Last reviewed: Oct 16, 2020)	
I204V	Uncertain significance(Last reviewed: Oct 12, 2019)	
S206P	Uncertain significance(Last reviewed: Sep 19, 2018)	
H207R	Uncertain significance(Last reviewed: Jan 16, 2019)	
H207Q	Uncertain significance(Last reviewed: Oct 29, 2020)	
I208V	Uncertain significance(Last reviewed: Oct 5, 2020)	
I208S	Uncertain significance(Last reviewed: Jun 17, 2020)	
Y210C	Uncertain significance(Last reviewed: Jan 13, 2020)	
F211L	Uncertain significance(Last reviewed: Nov 24, 2016)	
R212G	Uncertain significance(Last reviewed: Jun 13, 2020)	
R212C	Uncertain significance(Last reviewed: Oct 23, 2020)	
R212S	Uncertain significance(Last reviewed: Jul 25, 2018)	
R212L	Uncertain significance(Last reviewed: Jan 25, 2020)	
R212H	Uncertain significance(Last reviewed: May 1, 2021)	
R214C	Conflicting interpretations of pathogenicity(Last reviewed: Apr 28, 2021)	
R214H	Conflicting interpretations of pathogenicity(Last reviewed: Dec 2, 2020)	
D215G	Uncertain significance(Last reviewed: Jun 23, 2020)	
Y216C	Uncertain significance(Last reviewed: Nov 9, 2017)	
T217A	Uncertain significance(Last reviewed: Apr 30, 2019)	
T217S	Uncertain significance(Last reviewed: May 2, 2017)	
E218G	Uncertain significance(Last reviewed: Jan 9, 2018)	
L219S	Conflicting interpretations of pathogenicity(Last reviewed: Oct 23, 2020)	
Q222H	Uncertain significance(Last reviewed: Apr 24, 2019)	
V223I	Uncertain significance(Last reviewed: Apr 29, 2020)	
Y224C	Uncertain significance(Last reviewed: Jul 7, 2014)	
L225P	Uncertain significance(Last reviewed: Aug 2, 2019)	
L226P	Uncertain significance(Last reviewed: Oct 9, 2020)	

P227S	Uncertain significance(Last reviewed: Jun 30, 2020)	
P227L	Uncertain significance(Last reviewed: Apr 27, 2020)	
D228V	Uncertain significance(Last reviewed: Jun 6, 2020)	
D228G	Uncertain significance(Last reviewed: Oct 1, 2019)	
F229L	Uncertain significance(Last reviewed: May 17, 2019)	
L230F	Uncertain significance(Last reviewed: Oct 3, 2020)	
S231L	Uncertain significance(Last reviewed: Aug 25, 2018)	
E232D	Uncertain significance(Last reviewed: Nov 2, 2020)	
H233Y	Uncertain significance(Last reviewed: Mar 10, 2020)	
H233R	Uncertain significance(Last reviewed: Oct 5, 2020)	
K235E	Uncertain significance(Last reviewed: Jul 7, 2017)	
K235T	Uncertain significance(Last reviewed: Jan 25, 2021)	
K235N	Conflicting interpretations of pathogenicity(Last reviewed: Jun 16, 2021)	
V236D	Uncertain significance(Last reviewed: Nov 19, 2017)	
R237P	Uncertain significance(Last reviewed: Jul 8, 2020)	
R237Q	Uncertain significance(Last reviewed: Oct 26, 2020)	
L238R	Uncertain significance(Last reviewed: Aug 25, 2020)	
V239L	Uncertain significance(Last reviewed: Jun 13, 2018)	
V239M	Uncertain significance(Last reviewed: Jul 18, 2016)	
V239A	Uncertain significance(Last reviewed: Sep 30, 2019)	
V239E	Uncertain significance(Last reviewed: Sep 9, 2019)	
I240V	Uncertain significance(Last reviewed: Jan 21, 2017)	
I240L	Uncertain significance(Last reviewed: Sep 2, 2020)	
I240T	Uncertain significance(Last reviewed: Jan 25, 2021)	
V241M	Uncertain significance(Last reviewed: Feb 12, 2021)	
V241A	Uncertain significance(Last reviewed: Apr 18, 2020)	
D242N	Uncertain significance(Last reviewed: Oct 9, 2020)	
D242G	Uncertain significance(Last reviewed: Sep 12, 2019)	
G243S	Uncertain significance(Last reviewed: Sep 18, 2019)	
I244F	Uncertain significance(Last reviewed: Dec 7, 2018)	
I244V	Uncertain significance(Last reviewed: Apr 1, 2021)	
I244M	Uncertain significance(Last reviewed: Jun 28, 2019)	
A245V	Uncertain significance(Last reviewed: Jul 3, 2019)	
P247L	Uncertain significance(Last reviewed: Oct 9, 2020)	
F248L	Uncertain significance(Last reviewed: May 23, 2015)	
R249C	Uncertain significance(Last reviewed: May 25, 2020)	
R249H	Uncertain significance(Last reviewed: Dec 11, 2020)	
H250D	Uncertain significance(Last reviewed: Jul 30, 2019)	

H250Y	Uncertain significance(Last reviewed: Aug 27, 2020)	
H250R	Uncertain significance(Last reviewed: Mar 24, 2020)	
L252V	Uncertain significance(Last reviewed: Mar 9, 2015)	
L252Q	Uncertain significance(Last reviewed: Nov 12, 2019)	
D253G	Uncertain significance(Last reviewed: Dec 15, 2020)	
D254Y	Uncertain significance(Last reviewed: Jul 2, 2018)	
D254E	Uncertain significance(Last reviewed: Nov 29, 2018)	
L255P	Uncertain significance(Last reviewed: Apr 3, 2019)	
S256C	Uncertain significance(Last reviewed: Aug 14, 2020)	
L257V	Uncertain significance(Last reviewed: Aug 26, 2020)	
R258G	Uncertain significance(Last reviewed: Mar 13, 2017)	
R258C	Uncertain significance(Last reviewed: Mar 25, 2021)	
R258L	Uncertain significance(Last reviewed: Jan 11, 2019)	
R258P	Uncertain significance(Last reviewed: Dec 20, 2019)	
R258H	Pathogenic/Likely pathogenic(Last reviewed: Jul 13, 2021)	
T259S	Uncertain significance(Last reviewed: Aug 26, 2020)	
R260W	Uncertain significance(Last reviewed: Oct 19, 2020)	
R260Q	Uncertain significance(Last reviewed: Sep 17, 2020)	
R260P	Uncertain significance(Last reviewed: Sep 24, 2020)	
L261F	Uncertain significance(Last reviewed: Nov 29, 2018)	
L262V	Uncertain significance(Last reviewed: Sep 3, 2021)	
N263S	Uncertain significance(Last reviewed: Mar 4, 2019)	
G264S	Conflicting interpretations of pathogenicity(Last reviewed: Dec 8, 2020)	
G264V	Uncertain significance(Last reviewed: Oct 11, 2018)	
L265I	Uncertain significance(Last reviewed: Sep 24, 2020)	
L265V	Uncertain significance(Last reviewed: May 6, 2019)	
L265P	Uncertain significance(Last reviewed: Jul 14, 2016)	
A266D	Uncertain significance(Last reviewed: Aug 16, 2017)	
Q267H	Uncertain significance(Last reviewed: Aug 30, 2019)	
Q268K	Uncertain significance(Last reviewed: Sep 16, 2020)	
Q268R	Uncertain significance(Last reviewed: Jan 21, 2019)	
Q268H	Uncertain significance(Last reviewed: Apr 24, 2019)	
M269V	Uncertain significance(Last reviewed: Jan 26, 2018)	
M269L	Uncertain significance(Last reviewed: Oct 26, 2020)	
I270V	Uncertain significance(Last reviewed: Mar 29, 2019)	
I270M	Uncertain significance(Last reviewed: Mar 29, 2019)	
S271G	Uncertain significance(Last reviewed: Jan 13, 2017)	
S271N	Uncertain significance(Last reviewed: Jun 27, 2019)	

A273P	Uncertain significance(Last reviewed: Sep 8, 2019)	
A273E	Uncertain significance(Last reviewed: Mar 29, 2019)	
A273V	Uncertain significance(Last reviewed: Jun 1, 2016)	
N274S	Uncertain significance(Last reviewed: Sep 4, 2019)	
N274K	Uncertain significance(Last reviewed: Jan 13, 2018)	
N275D	Uncertain significance(Last reviewed: Aug 12, 2019)	
H276N	Uncertain significance(Last reviewed: Apr 28, 2018)	
H276Y	Uncertain significance(Last reviewed: Jun 2, 2020)	
H276P	Uncertain significance(Last reviewed: Sep 4, 2019)	
L278S	Uncertain significance(Last reviewed: Oct 19, 2016)	
A279P	Uncertain significance(Last reviewed: Oct 1, 2020)	
A279G	Uncertain significance(Last reviewed: Jul 18, 2019)	
V280I	Uncertain significance(Last reviewed: Oct 12, 2020)	
I281V	Uncertain significance(Last reviewed: Jul 23, 2019)	
T283S	Uncertain significance(Last reviewed: Nov 3, 2018)	
N284D	Uncertain significance(Last reviewed: Dec 11, 2019)	
N284S	Uncertain significance(Last reviewed: May 17, 2018)	
N284T	Uncertain significance(Last reviewed: Aug 17, 2016)	
Q285R	Uncertain significance(Last reviewed: Feb 6, 2019)	
Q285H	Uncertain significance(Last reviewed: Nov 15, 2019)	
M286V	Uncertain significance(Last reviewed: Mar 11, 2019)	
M286I	Uncertain significance(Last reviewed: Sep 9, 2020)	
T287P	Uncertain significance(Last reviewed: Nov 21, 2019)	
T287A	Benign/Likely benign(Last reviewed: Feb 1, 2021)	
T288A	Uncertain significance(Last reviewed: Mar 20, 2019)	
I290F	Uncertain significance(Last reviewed: Nov 20, 2019)	
I290T	Uncertain significance(Last reviewed: Sep 5, 2020)	
I290M	Uncertain significance(Last reviewed: Oct 21, 2019)	
D291G	Uncertain significance(Last reviewed: Mar 29, 2019)	
D291E	Uncertain significance(Last reviewed: Mar 26, 2020)	
R292G	Uncertain significance(Last reviewed: Mar 29, 2020)	
N293H	Uncertain significance(Last reviewed: Nov 29, 2018)	
N293S	Uncertain significance(Last reviewed: Sep 2, 2019)	
A295S	Uncertain significance(Last reviewed: May 1, 2018)	
A295T	Uncertain significance(Last reviewed: Sep 9, 2020)	
A295G	Uncertain significance(Last reviewed: Jun 26, 2020)	
L297R	Uncertain significance(Last reviewed: Nov 17, 2017)	
L297P	Uncertain significance(Last reviewed: Sep 11, 2020)	

V298L	Uncertain significance(Last reviewed: Dec 4, 2019)	
P299R	Uncertain significance(Last reviewed: Apr 3, 2019)	
P299L	Uncertain significance(Last reviewed: Aug 31, 2018)	
A300S	Uncertain significance(Last reviewed: Jun 17, 2020)	
A300E	Uncertain significance(Last reviewed: Apr 12, 2018)	
A300V	Uncertain significance(Last reviewed: Sep 17, 2020)	
G302R	Conflicting interpretations of pathogenicity(Last reviewed: Sep 17, 2020)	
G302V	Uncertain significance(Last reviewed: Sep 25, 2020)	
E303D	Uncertain significance(Last reviewed: Sep 29, 2019)	
S304I	Uncertain significance(Last reviewed: Aug 1, 2018)	
S304R	Uncertain significance(Last reviewed: May 28, 2019)	
G306R	Uncertain significance(Last reviewed: Sep 11, 2018)	
H307Y	Uncertain significance(Last reviewed: Dec 11, 2018)	
H307R	Uncertain significance(Last reviewed: Mar 13, 2019)	
A308S	Uncertain significance(Last reviewed: Oct 30, 2020)	
A308V	Uncertain significance(Last reviewed: May 21, 2015)	
A308G	Uncertain significance(Last reviewed: Apr 28, 2021)	
T310A	Uncertain significance(Last reviewed: Nov 23, 2020)	
T310I	Uncertain significance(Last reviewed: Dec 26, 2019)	
I311V	Uncertain significance(Last reviewed: May 30, 2019)	
I311T	Uncertain significance(Last reviewed: Dec 21, 2014)	
R312G	Uncertain significance(Last reviewed: Jun 7, 2020)	
R312W	Conflicting interpretations of pathogenicity(Last reviewed: May 6, 2021)	
R312Q	Uncertain significance(Last reviewed: Jul 20, 2020)	
H316Y	Uncertain significance(Last reviewed: Sep 15, 2015)	
D318Y	Uncertain significance(Last reviewed: Mar 15, 2018)	
D318N	Uncertain significance(Last reviewed: Oct 20, 2019)	
D318H	Uncertain significance(Last reviewed: Feb 14, 2019)	
R319Q	Conflicting interpretations of pathogenicity(Last reviewed: Oct 6, 2020)	
R319P	Uncertain significance(Last reviewed: Sep 17, 2014)	
K320E	Uncertain significance(Last reviewed: Feb 15, 2019)	
K320R	Uncertain significance(Last reviewed: Feb 10, 2014)	
K320N	Uncertain significance(Last reviewed: Feb 26, 2021)	
Q321R	Uncertain significance(Last reviewed: Apr 28, 2020)	
R322K	Uncertain significance(Last reviewed: Dec 3, 2019)	
R322T	Uncertain significance(Last reviewed: Sep 25, 2019)	
R322S	Uncertain significance(Last reviewed: Apr 24, 2019)	
L323W	Uncertain significance(Last reviewed: Jul 23, 2020)	

A324T	Uncertain significance(Last reviewed: Sep 26, 2019)	
T325A	Uncertain significance(Last reviewed: Sep 23, 2019)	
L326W	Uncertain significance(Last reviewed: Oct 2, 2019)	
L326S	Uncertain significance(Last reviewed: Jan 11, 2019)	
L326F	Uncertain significance(Last reviewed: Apr 3, 2019)	
Y327C	Uncertain significance(Last reviewed: Jun 15, 2018)	
K328E	Uncertain significance(Last reviewed: Sep 13, 2019)	
S329L	Uncertain significance(Last reviewed: Nov 17, 2019)	
P330S	Uncertain significance(Last reviewed: Jul 14, 2020)	
P330R	Uncertain significance(Last reviewed: Jul 8, 2020)	
P330L	Uncertain significance(Last reviewed: Aug 23, 2020)	
S331I	Uncertain significance(Last reviewed: Sep 2, 2014)	
S331R	Uncertain significance(Last reviewed: Jan 12, 2019)	
Q332K	Uncertain significance(Last reviewed: Jan 19, 2018)	
K333N	Uncertain significance(Last reviewed: Oct 29, 2020)	
E334K	Uncertain significance(Last reviewed: Jan 22, 2018)	
C335Y	Uncertain significance(Last reviewed: Feb 20, 2019)	
T336A	Uncertain significance(Last reviewed: Nov 2, 2018)	
T336P	Uncertain significance(Last reviewed: Nov 23, 2020)	
V337I	Uncertain significance(Last reviewed: Dec 6, 2018)	
F339S	Uncertain significance(Last reviewed: Oct 6, 2020)	
I341V	Uncertain significance(Last reviewed: Mar 25, 2019)	
P343S	Uncertain significance(Last reviewed: Jan 23, 2020)	
P343R	Uncertain significance(Last reviewed: Jan 1, 2016)	
P343L	Uncertain significance(Last reviewed: Dec 12, 2019)	
Q344H	Uncertain significance(Last reviewed: Nov 1, 2020)	
F346S	Uncertain significance(Last reviewed: May 29, 2020)	
D348Y	Uncertain significance(Last reviewed: Jun 20, 2017)	
D348V	Uncertain significance(Last reviewed: Oct 5, 2020)	
D348E	Uncertain significance(Last reviewed: Oct 16, 2020)	
T349A	Conflicting interpretations of pathogenicity(Last reviewed: Jul 9, 2019)	
T349I	Uncertain significance(Last reviewed: May 21, 2018)	
V350I	Uncertain significance(Last reviewed: Aug 14, 2020)	
V350F	Uncertain significance(Last reviewed: Sep 30, 2020)	
V351I	Uncertain significance(Last reviewed: Jul 25, 2020)	
T352N	Uncertain significance(Last reviewed: Sep 24, 2020)	
A354T	Uncertain significance(Last reviewed: Jun 13, 2020)	
A354V	Uncertain significance(Last reviewed: Oct 25, 2020)	

C355R	Uncertain significance(Last reviewed: Jun 1, 2020)	
C355Y	Uncertain significance(Last reviewed: Jun 15, 2020)	
S356L	Uncertain significance(Last reviewed: Mar 7, 2019)	
Q358E	Uncertain significance(Last reviewed: Oct 9, 2020)	
Q358L	Uncertain significance(Last reviewed: Sep 5, 2018)	
Q358R	Uncertain significance(Last reviewed: May 14, 2019)	
S362F	Uncertain significance(Last reviewed: Jul 19, 2019)	
S364R	Uncertain significance(Last reviewed: Dec 5, 2019)	
S364G	Conflicting interpretations of pathogenicity(Last reviewed: Sep 21, 2020)	
T365P	Uncertain significance(Last reviewed: Dec 21, 2016)	
T365S	Conflicting interpretations of pathogenicity(Last reviewed: Jun 26, 2019)	
T365I	Uncertain significance(Last reviewed: Feb 23, 2017)	
R366W	Uncertain significance(Last reviewed: Oct 15, 2020)	
R366P	Uncertain significance(Last reviewed: Sep 11, 2020)	
R366Q	Uncertain significance(Last reviewed: Oct 1, 2020)	
K367Q	Uncertain significance(Last reviewed: Nov 5, 2018)	
R368W	Uncertain significance(Last reviewed: May 19, 2021)	
R368Q	Uncertain significance(Last reviewed: Nov 18, 2020)	
S369L	Uncertain significance(Last reviewed: Jul 12, 2020)	
R370Q	Uncertain significance(Last reviewed: May 14, 2021)	
D371E	Uncertain significance(Last reviewed: Nov 13, 2018)	
E373K	Uncertain significance(Last reviewed: May 6, 2020)	
E373A	Uncertain significance(Last reviewed: Sep 13, 2019)	
E374K	Uncertain significance(Last reviewed: Aug 15, 2018)	
E375K	Uncertain significance(Last reviewed: Mar 18, 2019)	
L376I	Uncertain significance(Last reviewed: Aug 21, 2020)	

Supplementary Table S1. RAD51C missense variants reported in ClinVar as of October 2021 (ncbi.nlm.nih.gov/clinvar), obtained mostly through clinical sequencing. All variants are germline in origin. Two of the variants are considered to be benign/likely benign and 7 pathogenic/likely pathogenic. Most of the rest of the nearly 600 variants are considered to be of uncertain significance, although 19 have conflicting interpretations of pathogenicity. All reported variants are germline.

Supplemental Table S2. RAD51C cancer variants.

Variant	Cancer Type	Allele origin	Source	ClinVar
M1T	KIRC	somatic	MSK	
R2C	READ	somatic	MSK	
G3R	EOC, BRCA	germline	(1,2)	ClinVar
T5M	BRCA	somatic	MSK, COSMIC, (2)	ClinVar
F6S	UCEC	somatic	MSK	
F6L	LUAD	somatic	MSK,	ClinVar
R7C	COAD, LUAD	somatic	MSK, COSMIC	ClinVar
F8L	OS	somatic	(3)	ClinVar
E9D	COAD	somatic	COSMIC, TCGA	
Q11H	EHCC	somatic	MSK	
Q11R	EOC	germline	(2)	ClinVar
R12Q	CESC	somatic	MSK, COSMIC	ClinVar
D13N	UCEC, ALL/LBL	somatic	MSK, COSMIC, (4)	ClinVar
V15M	UCEC	somatic	TCGA	
S16N	THYM	somatic	TCGA	ClinVar
P18R	HNSC	somatic	TCGA	ClinVar
P18S	SCC	somatic	COSMIC	ClinVar
P21A	BRCA, LUAD	somatic	MSK, COSMIC, TCGA	ClinVar
P21S	BRCA, LUAD	somatic	MSK, COSMIC, TCGA	ClinVar
P21T	COAD, BLCA	somatic	MSK, COSMIC, TCGA	
A22T	PAAD	somatic	MSK	
V23L	LUAD	somatic	MSK	
R24L	LUSC	somatic	TCGA	ClinVar
R24P	PRAD	somatic	MSK	
K26M	EOC	germline	(2)	ClinVar
K26N	LUSC	somatic	TCGA	
L27V	LUAD	somatic	MSK	
L27P	EOC	germline	(2)	ClinVar
S29F	USC	somatic	MSK	ClinVar
S29P	LUAD	somatic	MSK, COSMIC	
A30E	BRCA	germline	(5,6)	
Q33H	UCEC	somatic	MSK	ClinVar
E36D	NOS	somatic	MSK	
E36K	BRCA	germline	(5,6)	ClinVar
E37K	MCC	somatic	MSK	
V41M	COAD	somatic	MSK	ClinVar
P43L	SKCM, MPM	somatic	MSK, COSMIC	ClinVar
P43S	EOC	germline	(2)	ClinVar
S44C	BRCA	somatic	MSK	
E45D	EHCC, CHOL	somatic	COSMIC	ClinVar
E45G	BRCA	germline	MSK, (5,6)	ClinVar
G51V	LUAD	somatic	COSMIC	ClinVar
I52L	UCEC	somatic	TCGA	ClinVar

S53C	SCC	somatic	COSMIC	ClinVar
A57V	GBM	somatic	(7)	
E59K	CESC, GBM	somatic	MSK, COSMIC, TCGA	
I63S	LUAD	somatic	TCGA	
E67G	BRCA	germline	(8)	ClinVar
E67K	EOC	germline	(2)	
C68F	LUAD	somatic	MSK, COSMIC	
N71D	UCEC	somatic	TCGA	
N71K	EOC	germline	(2)	
R74K	BRCA	somatic	MSK, TCGA	
Y75C	NEC	somatic	MSK	ClinVar
G77D	ALL/LBL, SKCM	somatic	MSK, COSMIC	ClinVar
E80K	BRCA	somatic	MSK, TCGA	
E80Q	BLCA, SCC	somatic	MSK, TCGA, COSMIC	
H82N	EOC	germline	(2)	
K83N	COAD, READ	somatic	MSK, COSMIC	ClinVar
K84M	SCC	somatic	TCGA	
K84R	COAD	somatic	COSMIC	
K84N	EOC, COAD	germline, somatic	(2), COSMIC	ClinVar
A87S	GBM	somatic	(4)	ClinVar
A87T	COAD	somatic	COSMIC	ClinVar
E89K	BLCA	somatic	MSK	ClinVar
L91F	EOC	germline	(2)	ClinVar
E92D	BRCA	somatic	MSK	
E92K	PAAD	somatic	TCGA	ClinVar
E94G	NOS	somatic	MSK	
T96S	LUAD	somatic	MSK	ClinVar
Q97H	UCEC	somatic	MSK	
G98S	COAD, READ	somatic	MSK, COSMIC	
T102I	MCC	somatic	MSK	ClinVar
F103V	BRCA	germline	(9)	ClinVar
S105L	LUAD	somatic	MSK, COSMIC	
A106T	COAD	somatic	MSK	
L107P	THCA	somatic	COSMIC	
D108N	GBM	somatic	TCGA	
D108Y	COAD, READ	somatic	MSK, COSMIC	
L111P	NB	somatic	MSK	
G112A	OS	somatic	(4,10)	ClinVar
G112R	SKCM	somatic	COSMIC	
G112V	EOC	germline	(2)	ClinVar
G113S	BRCA	somatic	COSMIC, TCGA, MSK	
M118I	BRCA, SCC	somatic	TCGA, COSMIC	ClinVar
T120I	UCEC	somatic	MSK	
T120A	EOC	germline	(2)	

T121R	EOC	somatic	This study	
G125V	BRCA	germline	(1)	ClinVar
A126T	EOC, BRCA	germline	MSK, COSMIC, (1,2,5,6,9,11-14)	ClinVar
P127Q	ALL/LBL	somatic	(10,15)	
G130A	BRCA	somatic	MSK	ClinVar
T132P	EOC	germline	(2,14,16)	ClinVar
Q133K	EOC	germline	This study (2,14)	ClinVar
L134S	MCT	somatic	(10)	ClinVar
C135R	BRCA	germline	(6,8)	
C135Y	EOC, BRCA	germline	(6,9)	
M136I	LUAD, EOC	somatic	MSK, (2)	ClinVar
M136L	LUAD	germline	COSMIC	ClinVar
L138F	EOC, BRCA	germline	(1,6)	ClinVar
A139T	RCC	somatic	MSK	ClinVar
V140G	EOC	germline	(2)	
D141N	BLCA	somatic	MSK	ClinVar
D141H	BRCA	unknown	TCGA	
Q143R	BRCA	germline	(2,5,6)	ClinVar
I144M	UPS/SCS	somatic	MSK	ClinVar
I144T	EOC	germline	(2)	ClinVar
G149R	BLCA	somatic	MSK	
G150A	LUAD	somatic	MSK	
V151G	LMS	somatic	MSK	
V151M	AOD, GBM	somatic	MSK, COSMIC	ClinVar
A152T	RMS, MMT	somatic	COSMIC	ClinVar
G153D	BRCA	germline	(11,12)	ClinVar
G153S	HCC	somatic	COSMIC	
A155T	SKCM	somatic	MSK, COSMIC	ClinVar
A155V	ACC	somatic	TCGA	
F157C	UCEC, ESCA	somatic	MSK	ClinVar
I158F	MB	somatic	(17)	
D159N	BRCA	germline	(1)	ClinVar
T160A	COAD	somatic	MSK	
E161D	LUAD	somatic	MSK, COSMIC	ClinVar
G162A	EOC	somatic	MSK	
G162E	EOC, BRCA	germline	MSK, (2)	ClinVar
G162R	SKCM	somatic	MSK, TCGA, COSMIC	
S163R	STAD	somatic	MSK, COSMIC	ClinVar
M165L	EOC	germline	(2)	
V166G	EOC	germline	(2)	
D167N	BLCA, PRAD	somatic	COSMIC, TCGA	
D167Y	THCA	somatic	MSK	
R168K	BLCA	somatic	MSK, COSMIC	
V169A	EOC, BRCA	germline	(1,2)	ClinVar
V170G	EOC	germline	(2)	
V170I	COAD	somatic	MSK, COSMIC	ClinVar
D171H	HCC	somatic	COSMIC	
L172V	CESC	somatic	TCGA	ClinVar

L172I	COAD	somatic	COSMIC	
T174S	EOC	germline	(2)	
A175T	SCC	somatic	COSMIC	ClinVar
A175V	COAD	somatic	MSK	
Q178E	EOC, BLCA	somatic	MSK, COSMIC	
H179Y	UCEC	somatic	MSK	
Q181R	EOC	germline	MSK	ClinVar
L182R	EOC	somatic	MSK	
I183L	MPM	somatic	MSK	
A184E	NEC	somatic	MSK	
K188N	BRCA	germline	(8)	ClinVar
G189R	EOC	germline	(2)	ClinVar
G189V	SCC	somatic	MSK	
E190G	LUAD, NSCLC	somatic	MSK	
R193L	EOC	Reversion	(18)	
R193Q	UCEC, NSCLC	somatic	MSK, TCGA	ClinVar
R193W	EOC	Reversion	(18)	
K194R	HNSC	somatic	MSK	
E197D	GBM	somatic	TCGA	
L201F	BLCA	somatic	MSK, COSMIC	
L201V	BLCA	somatic	MSK	ClinVar
D202V	SKCM	somatic	MSK, COSMIC	
N203I	BLCA	somatic	MSK	
N203D	EOC	germline	(2)	ClinVar
I204V	BLCA	somatic	MSK	ClinVar
L205P	MCT	somatic	(10)	
L205V	COAD, READ	somatic	MSK	
L205F	BRCA, LUSC, SKCM	somatic	MSK, TCGA, COSMIC	
H207Y	LUAD	somatic	MSK	
H207D	BRCA	somatic	MSK	
H207R	EOC	germline	(2)	ClinVar
I208V	NSCLC	somatic	MSK	ClinVar
Y209C	LUAD	somatic	MSK, COSMIC	
R212H	COAD	somatic	MSK, COSMIC	ClinVar
R212C	UCEC, LUAD	somatic	MSK	ClinVar
C213Y	CHOL	somatic	MSK	
R214H	ESCA	somatic	MSK, COSMIC	ClinVar
R214C	COAD	somatic	This study, MSK, COSMIC, (11)	ClinVar
E218K	UCEC	somatic	MSK	
E218D	UCEC	somatic	MSK	
L219S	EOC, BRCA	germline	(6,12)	ClinVar
Q222R	UCEC	somatic	MSK	
V223A	UCEC	somatic	TCGA	
Y224H	BLCA	somatic	MSK, TCGA	

L226F	BLCA	somatic	MSK	
L226P	EOC	germline	(2)	ClinVar
P227L	SKCM	somatic	MSK	ClinVar
D228H	THCA	somatic	MSK	
D228Y	LUAD	somatic	MSK	
F229L	MCT	somatic	(10)	ClinVar
L230F	BRCA, SKCM	somatic	MSK, COSMIC	ClinVar
S231L	BRCA, LUAD	somatic	MSK, TCGA	ClinVar
H233Q	SKCM, HNSC, PAAD	somatic	MSK	
K235N	BRCA	somatic	MSK	ClinVar
K235Q	UCEC	somatic	MSK, COSMIC	
R237L	LUAD	somatic	MSK	
P247L	SKCM	somatic	MSK, COSMIC	ClinVar
R249C	BRCA, SKCM, DA	somatic	MSK, COSMIC, TCGA, (13)	ClinVar
R249H	EOC, LUSC, KIRC	germline	COSMIC, (2)	ClinVar
R249S	GBM	somatic	MSK	
H250Y	GBM	somatic	Mayo Clinic	ClinVar
D251G	PAAD	somatic	MSK	
D253N	NOS	germline	(19)	
L257V	HCC	somatic	COSMIC	ClinVar
R258H	COAD, GBM, PRAD	germline, somatic	MSK, COSMIC, (20)	ClinVar
R260Q	UCEC	somatic	MSK	ClinVar
R260W	PRAD	somatic	MSK	ClinVar
L262V	EOC, PRAD	germline	COSMIC, (2,14)	ClinVar
G264D	COAD	somatic	MSK, (10)	
G264S	EOC, BRCA, Teratoma, PRAD	germline, somatic	MSK, COSMIC, (1,2)	ClinVar
G264V	BRCA	germline	(1)	ClinVar
A266T	UCEC	somatic	MSK	
N275S	PRAD	somatic	MSK	
R277T	LUAD	somatic	MSK	
A279D	UCEC	somatic	TCGA	
A279P	EOC, ESCA	somatic	MSK, (2)	ClinVar
A279V	UCEC	somatic	COSMIC	
T283A	MCT	somatic	(10)	
T283I	MCT	somatic	(10)	
T287A	EOC, BRCA, PRAD	germline	COSMIC, (1,2,5,6,9,11-14)	ClinVar
K289N	LUAD	somatic	MSK	
I290T	BRCA	germline	(5,6)	ClinVar
D291Y	COAD	somatic	MSK, COSMIC	

D291V	EOC, HCC, LUAD, COAD	germline, somatic	MSK, (2)	
R292K	AOD	somatic	MSK, COSMIC	
A295G	MCT	somatic	(10)	ClinVar
A295T	UCEC	somatic	MSK	ClinVar
A295V	SKCM	somatic	MSK	
L297I	NOS	somatic	MSK	
L297R	GBM	somatic	MSK	ClinVar
P299S	BCC	somatic	MSK	
G302E	SKCM	somatic	MSK	
W305L	THCA	somatic	TCGA	
R312L	SKCM	somatic	TCGA	
R312Q	GBM	somatic	MSK	ClinVar
R312W	EOC, COAD	somatic, germline	This Study, MSK, COSMIC, TCGA (21)	ClinVar
H316N	COAD	somatic	MSK	
H316Y	BRCA	somatic	MSK, COSMIC	ClinVar
D318Y	LUAD	somatic	MSK	ClinVar
D318E	BRCA	somatic	MSK	
D318N	EOC	germline	(2)	ClinVar
R319L	HCC	somatic	COSMIC	
R319Q	EOC, COAD, UCEC	somatic, germline	MSK, COSMIC, (2)	ClinVar
K320M	LUAD	somatic	COSMIC	
A324T	COAD	somatic	TCGA	ClinVar
A324V	UCEC	somatic	MSK	
S329L	LUSC	somatic	MSK	ClinVar
P330H	BLCA	somatic	COSMIC	
P330S	SKCM	somatic	MSK, COSMIC	ClinVar
S331N	MCT	somatic	(10)	
Q332P	SCC	somatic	MSK	
T336P	EOC	germline	(2)	ClinVar
V337L	SCLC	somatic	MSK	
F339L	BLCA	somatic	MSK	
Q340E	GBM	somatic	TCGA	
Q340K	SCC	somatic	COSMIC	
I341M	BRCA	somatic	MSK, TCGA	
P343S	UCEC	somatic	MSK	ClinVar
Q344E	BLCA	somatic	(22)	
G345R	GBM, SKCM	somatic	MSK, TCGA	
R347K	UCEC	somatic	TCGA	
D348V	ULE	germline	MSK	ClinVar
D348Y	UCEC	somatic	MSK	ClinVar
T349A	BRCA, COAD	somatic	MSK, TCGA	ClinVar
V350I	STAD	somatic	TCGA	ClinVar
T352S	NOS	somatic	MSK	
S353T	BRCA	somatic	MSK	

A354T	COAD	somatic	MSK, COSMIC	ClinVar
A354V	EOC	germline	(2)	ClinVar
S356L	BLCA	somatic	MSK	ClinVar
L357S	UCEC	somatic	TCGA	
Q358K	CHOL	somatic	MSK	
E360A	LUAD	somatic	MSK	
E360Q	BRCA	somatic	COSMIC	
S362F	SKCM, BCC	somatic	MSK	ClinVar
L363M	SKCM	somatic	MSK	
S364G	EOC	germline	(2)	ClinVar
T365N	SCC	somatic	COSMIC	
R366Q	EOC, BRCA, SKCM	germline	COSMIC, (1)	ClinVar
R366W	NOS	germline	(19)	ClinVar
R368Q	ECUC, HCC, COAD	somatic	MSK, COSMIC	ClinVar
R368W	COAD, MCC, SKCM	somatic	MSK, COSMIC	ClinVar
S369P	COAD	somatic	MSK	
R370Q	UCEC, MDS	somatic	MSK	ClinVar
D371Y	UCEC	somatic	MSK	
P372S	GBM	somatic	Mayo Clinic	
E374K	SKCM	somatic	COSMIC	ClinVar
E375K	GBM	somatic	MSK	ClinVar

Supplementary Table S2. RAD51C cancer variants identified from the following sources: Memorial Sloan Kettering Cancer Center (MSK), Catalogue of Somatic Mutations in Cancer (COSMIC), The Cancer Genome Atlas (TCGA), the indicated references (see **Fig. 1**), and patients in this study. Variants found in breast or ovarian tumors are colored pink; Variants found in other cancer types are colored black. Those variants also reported in ClinVar are indicated.

MSK clinical sequencing through MSK-IMPACT and related platforms is performed by the MSK Molecular Diagnostics Service and the Marie-Josée and Henry R. Kravis Center for Molecular Oncology in the Department of Pathology. MSK-IMPACT (Integrated Mutation Profiling of Actionable Cancer Targets) is a targeted tumor-sequencing test available to MSK patients. It currently analyzes 505 genes, although earlier versions involved analysis smaller number (~400). For 99% of cases, a matched normal is sequenced and used in the mutation calling to infer which mutations are somatic. The vast majority of MSK-IMPACT mutations are somatic variants. Germline mutations are reported for patients that have consented; however, it is limited to a subset of genes, and, with a few exceptions, only known or likely pathogenic variants are reported. TCGA involved sequencing of primary cancer samples and matched

normal and also evolved during the effort but analyzed a much larger set of genes. COSMIC contains somatic mutation from TGCA and other sources.

Cancer abbreviations:

AA	Astrocytoma
ACC	Adrenocortical Carcinoma
ALL/LB	T-Lymphoblastic Leukemia/Lymphoma
AOD	Anaplastic Oligodendroglioma
BCC	Basal Cell Carcinoma
BLCA	Bladder Urothelial Carcinoma
BRCA	Breast invasive carcinoma/Breast cancer
CESC	Cervical squamous cell carcinoma and endocervical adenocarcinoma
CHOL	Cholangiocarcinoma
COAD	Colon Adenocarcinoma
DA	Duodenal Adenocarcinoma
EHCC	Extrahepatic Cholangiocarcinoma
EOC	Epithelial Ovarian Carcinoma
ESCA	Esophageal carcinoma
GBC	Gallbladder Cancer
GBM	Glioblastoma multiforme
HCC	Hepatocellular Carcinoma/Liver Cancer
HNSC	Head and Neck Squamous Cell Carcinoma
KIRC	Kidney renal clear cell carcinoma
LMS	Leiomyosarcoma
LUAD	Lung adenocarcinoma
LUSC	Lung Squamous Cell Carcinoma
MB	Medulloblastoma
MCC	Merkel Cell Carcinoma
MCT	Mixed Cancer Types
MDS	Myelodysplastic Syndromes
MMMT	Uterine Malignant Mixed Mullerian Tumor
MPM	Malignant Pleural Mesothelioma
NB	Neuroblastoma
NEC	Neuroendocrine cancer/Islet cell carcinoma
NOS	Not Otherwise Described
NSCLC	Non-small-cell lung carcinoma
OS	Osteosarcoma
PAAD	Pancreatic Adenocarcinoma
PRAD	Prostate Adenocarcinoma
RCC	Renal Cell Carcinoma
READ	Rectum adenocarcinoma
RMS	Rhabdomyosarcoma
SCC	Squamous Cell Carcinoma
SCLC	Small Cell Lung Cancer
SCS	Spindle Cell Sarcoma
SKCM	Skin Cutaneous Melanoma, Melanoma
STAD	Stomach adenocarcinoma
THCA	Thyroid carcinoma
THYM	Thymoma
UCEC	Uterine (Corpus) Endometrial Carcinoma
UPS	Undifferentiated Pleomorphic Sarcoma

USC Uterine Carcinosarcoma
ULE Uterine Leiomyoma

References:

1. Meindl A, Hellebrand H, Wiek C, Erven V, Wappenschmidt B, Niederacher D, *et al.* Germline mutations in breast and ovarian cancer pedigrees establish RAD51C as a human cancer susceptibility gene. *Nat Genet* **2010**;42(5):410-4.
2. Song H, Dicks E, Ramus SJ, Tyrer JP, Intermaggio MP, Hayward J, *et al.* Contribution of Germline Mutations in the RAD51B, RAD51C, and RAD51D Genes to Ovarian Cancer in the Population. *J Clin Oncol* **2015**;33(26):2901-7.
3. Oberg JA, Glade Bender JL, Sulis ML, Pendrick D, Sireci AN, Hsiao SJ, *et al.* Implementation of next generation sequencing into pediatric hematology-oncology practice: moving beyond actionable alterations. *Genome Med* **2016**;8(1):133.
4. Rokita JL, Rathil KS, Cardenas MF, Upton KA, Jayaseelan J, Cross KL, *et al.* Genomic Profiling of Childhood Tumor Patient-Derived Xenograft Models to Enable Rational Clinical Trial Design. *Cell Rep* **2019**;29(6):1675-89 e9.
5. Romero A, Perez-Segura P, Tosar A, Garcia-Saenz JA, Diaz-Rubio E, Caldes T, *et al.* A HRM-based screening method detects RAD51C germ-line deleterious mutations in Spanish breast and ovarian cancer families. *Breast Cancer Res Treat* **2011**;129(3):939-46.
6. Osorio A, Endt D, Fernandez F, Eirich K, de la Hoya M, Schmutzler R, *et al.* Predominance of pathogenic missense variants in the RAD51C gene occurring in breast and ovarian cancer families. *Hum Mol Genet* **2012**;21(13):2889-98.
7. Johnson BE, Mazor T, Hong C, Barnes M, Aihara K, McLean CY, *et al.* Mutational analysis reveals the origin and therapy-driven evolution of recurrent glioma. *Science* **2014**;343(6167):189-93.
8. Ding YC, Adamson AW, Steele L, Bailis AM, John EM, Tomlinson G, *et al.* Discovery of mutations in homologous recombination genes in African-American women with breast cancer. *Fam Cancer* **2018**;17(2):187-95.
9. Sanchez-Bermudez AI, Sarabia-Meseguer MD, Garcia-Aliaga A, Marin-Vera M, Macias-Cerrolaza JA, Henarejos PS, *et al.* Mutational analysis of RAD51C and RAD51D genes in hereditary breast and ovarian cancer families from Murcia (southeastern Spain). *Eur J Med Genet* **2018**;61(6):355-61.
10. Ghandi M, Huang FW, Jane-Valbuena J, Kryukov GV, Lo CC, McDonald ER, 3rd, *et al.* Next-generation characterization of the Cancer Cell Line Encyclopedia. *Nature* **2019**;569(7757):503-8.
11. Clague J, Wilhoite G, Adamson A, Bailis A, Weitzel JN, Neuhausen SL. RAD51C germline mutations in breast and ovarian cancer cases from high-risk families. *PLoS One* **2011**;6(9):e25632.
12. Blanco A, Gutierrez-Enriquez S, Santamarina M, Montalban G, Bonache S, Balmana J, *et al.* RAD51C germline mutations found in Spanish site-specific breast cancer and breast-ovarian cancer families. *Breast Cancer Res Treat* **2014**;147(1):133-43.
13. Thompson ER, Boyle SE, Johnson J, Ryland GL, Sawyer S, Choong DY, *et al.* Analysis of RAD51C germline mutations in high-risk breast and ovarian cancer families and ovarian cancer patients. *Hum Mutat* **2012**;33(1):95-9.
14. Cunningham JM, Cicek MS, Larson NB, Davila J, Wang C, Larson MC, *et al.* Clinical characteristics of ovarian cancer classified by BRCA1, BRCA2, and RAD51C status. *Sci Rep* **2014**;4:4026.
15. Kaisary AV, Grant RW. "Beehive on the bladder": an indication of colovesical disease. *Br J Urol* **1984**;56(1):35-7.

16. Sullivan MR, Prakash R, Rawal Y, Wang W, Sung P, Radke MR, *et al.* Long-term survival of an ovarian cancer patient harboring a RAD51C missense mutation. *Cold Spring Harb Mol Case Stud* **2021**;7(2) doi 10.1101/mcs.a006083.
17. Grobner SN, Worst BC, Weischenfeldt J, Buchhalter I, Kleinheinz K, Rudneva VA, *et al.* The landscape of genomic alterations across childhood cancers. *Nature* **2018**;555(7696):321-7.
18. Kondrashova O, Nguyen M, Shield-Artin K, Tinker AV, Teng NNH, Harrell MI, *et al.* Secondary Somatic Mutations Restoring RAD51C and RAD51D Associated with Acquired Resistance to the PARP Inhibitor Rucaparib in High-Grade Ovarian Carcinoma. *Cancer Discov* **2017**;7(9):984-98.
19. Jonson L, Ahlborn LB, Steffensen AY, Djursby M, Ejlertsen B, Timshel S, *et al.* Identification of six pathogenic RAD51C mutations via mutational screening of 1228 Danish individuals with increased risk of hereditary breast and/or ovarian cancer. *Breast Cancer Res Treat* **2016**;155(2):215-22.
20. Vaz F, Hanenberg H, Schuster B, Barker K, Wiek C, Erven V, *et al.* Mutation of the RAD51C gene in a Fanconi anemia-like disorder. *Nat Genet* **2010**;42(5):406-9.
21. Gayarre J, Martin-Gimeno P, Osorio A, Paumard B, Barroso A, Fernandez V, *et al.* Characterisation of the novel deleterious RAD51C p.Arg312Trp variant and prioritisation criteria for functional analysis of RAD51C missense changes. *Br J Cancer* **2017**;117(7):1048-62 doi 10.1038/bjc.2017.286.
22. Faltas BM, Prandi D, Tagawa ST, Molina AM, Nanus DM, Sternberg C, *et al.* Clonal evolution of chemotherapy-resistant urothelial carcinoma. *Nat Genet* **2016**;48(12):1490-9.

Supplementary Table S3. RAD51 population variants from gnomAD.

Variant	Population	Allele Count	Total Frequency
R2G	Latino	1/251270	3.98E-06
R2S	Latino	1/251270	3.98E-06
R2C	European	1/251270	3.98E-06
G3R	Most: European	11/282672	3.89E-05
T5S	East Asian	2/251382	7.96E-06
T5P	European	1/251382	3.98E-06
T5M	European	9/251372	3.58E-05
T5R	European	1/251372	3.98E-06
F6L	European	1/251398	3.98E-06
F6Y	European	1/251416	3.98E-06
R7S	African	1/251408	3.98E-06
R7G	European	1/251408	3.98E-06
R7C	South Asian	3/251408	1.19E-05
F8I	South Asian	1/251434	3.98E-06
M10L	African	1/31382	3.19E-05
M10R	European	2/251448	7.95E-06
M10I	European	1/251450	3.98E-06
Q11R	European	1/251450	3.98E-06
R12G	European	1/251456	3.98E-06
R12W	Most: African	2/251456	7.95E-06
R12P	South Asian	2/251448	7.95E-06
D13G	European	1/251462	3.98E-06
S16G	Most: European	5/251452	1.99E-05
P18S	Most: South Asian	10/251454	3.98E-05
P18L	European	3/251452	1.19E-05
S20F	Latino	1/251470	3.98E-06
P21A	South Asian	1/251466	3.98E-06
V23M	East Asian	1/251470	3.98E-06
R24Q	East Asian	1/251464	3.98E-06
V25M	South Asian	2/251464	7.95E-06
K26T	European	2/251476	7.95E-06
K26M	European	2/282878	7.97E-06
S29F	South Asian	1/251474	3.98E-06
A30V	Latino	1/251464	3.98E-06
G31R	South Asian	1/251446	3.98E-06
G31E	European	2/251464	7.95E-06
T34I	South Asian	1/251470	3.98E-06

A34T	South Asian	1/251468	3.98E-06
E36K	European	4/251458	1.59E-05
L39V	European	1/251416	3.98E-06
V41M	South Asian	2/251432	7.95E-06
V41L	African	1/31398	3.18E-05
P43S	Latino	1/251412	3.98E-06
P43L	East Asian	2/251416	7.95E-06
S44A	Latino	1/251396	3.98E-06
E45G	Most: Ashkenazi Jewish	15/251372	5.97E-05
E45D	African	1/215336	3.98E-06
E49K	East Asian	1/251294	3.98E-06
E49G	European	1/250514	3.99E-06
G51V	South Asian	1/250872	3.99E-06
A55V	Most: European	4/282586	1.42E-05
I63M	African	1/31404	3.18E-05
I64V	East Asian	1/251426	3.98E-06
I64F	European	1/251426	3.98E-06
R65G	European	1/251436	3.98E-06
E67G	Most: African	11/282858	3.89E-05
T70P	South Asian	1/251452	3.98E-06
K72E	European	2/251460	7.95E-06
A76G	Latino	1/251462	3.98E-06
G77A	East Asian	1/251456	3.98E-06
T78I	East Asian	16/251456	6.36E-05
K83R	European	1/251458	3.98E-06
K83T	Latino	1/251458	3.98E-06
K84N	European	2/251460	7.95E-06
C85G	East Asian	1/251464	3.98E-06
E89K	Latino	1/251462	3.98E-06
E92K	European	1/251466	3.98E-06
E94K	European	1/251472	3.98E-06
H95N	Latino	1/251466	3.98E-06
T96S	European	2/282856	7.07E-06
T102S	European	1/251454	3.98E-06
L107V	South Asian	1/251418	3.98E-06
D109Y	European	1/251358	3.98E-06
L111F	Latino	3/251342	1.19E-05
G112E	Latino	1/251296	3.98E-06
G112A	European	1/251296	3.98E-06

G114R	African	1/31384	3.19E-05
V115A	Other	1/251030	3.98E-06
C124S	Latino	2/250522	7.98E-06
G125S	European	1/250004	4.00E-06
A126T	Most: European	981/281388	3.49E-03
G130R	South Asian	1/248270	4.03E-06
K131I	European	1/248530	4.02E-06
K131R	South Asian	2/248530	8.05E-06
Q133G	African	2/279268	7.16E-06
L134S	East Asian	1/247194	4.05E-06
C135A	South Asian	1/247152	4.05E-06
M136L	East Asian	3/251476	1.19E-05
M136I	Most: European	3/282870	1.06E-05
L138F	European	1/251476	3.98E-06
V140L	African	1/31400	3.18E-05
V140G	European	1/251480	3.98E-06
Q143R	European	9/251480	3.58E-05
I144L	Latino	1/251478	3.98E-06
I144T	Most: European	16/282878	5.66E-05
P145L	African	1/31386	3.19E-05
C147Y	European	1/251488	3.98E-06
V151M	South Asian	5/251484	1.99E-05
V151L	African	1/31402	3.18E-05
A152S	European	1/251486	3.98E-06
G153D	Most: Latino	2/251462	7.95E-06
G154K	Latino	2/251458	7.95E-06
A155T	European	1/251454	3.98E-06
V156D	European	1/242482	4.12E-06
F157I	European	1/251464	3.98E-06
I158T	East Asian	1/251464	3.98E-06
E161Q	South Asian	4/251466	1.59E-05
G162E	European	1/251482	3.98E-06
S163G	Most: East Asian	2/251474	7.95E-06
S163N	Latino	1/251476	3.98E-06
F164L	Most: Latino	10/251476	3.98E-05
V166A	European	2/251456	7.95E-06
R168G	Latino	1/251478	3.98E-06
R168K	Latino	1/251478	3.98E-06
V169A	European	42/282840	1.48E-04

L172V	Latino	1/251462	3.98E-06
A175T	Most: European	6/251468	2.39E-05
A175V	African	1/31394	3.19E-05
H179Q	Latino	5/251476	1.99E-05
Q181H	South Asian	1/251472	3.98E-06
I183V	Most: European	3/251470	1.19E-05
I183T	European	2/251468	7.95E-06
A184T	European	2/251468	7.95E-06
K188M	Latino	7/282878	2.47E-05
G189R	European	1/251472	3.98E-06
G189A	South Asian	1/251470	3.98E-06
E190K	European	1/251456	3.98E-06
R193Q	Most: European	4/282586	1.42E-05
F199L	South Asian	1/251262	3.98E-06
L201V	Ashkenazi Jewish	3/251262	1.19E-05
N203D	Latino	2/251262	7.96E-06
H207R	European	1/31390	3.19E-05
H207Q	European	3/251246	1.19E-05
I208V	European	3/251238	1.19E-05
I208M	European	1/251250	3.98E-06
R212C	Most: South Asian	9/282638	3.18E-05
R212H	Most: East Asian	25/282612	8.85E-05
R214C	Most: African	22/282622	7.78E-05
R214H	South Asian	2/251240	7.96E-06
D215Y	European	1/31388	3.19E-05
D215G	European	1/251266	3.98E-06
Y216F	European	4/251256	1.59E-05
L219S	Most: Latino	2/251286	7.96E-06
F229L	European	2/251196	7.96E-06
L230F	South Asian	1/251194	3.98E-06
H233R	Most: South Asian	6/251138	2.39E-05
K235T	South Asian	4/251054	1.59E-05
K235N	European	1/251038	3.98E-06
R237Q	European	1/251386	3.98E-06
R237P	South Asian	1/251386	3.86E-06
V239L	South Asian	1/251408	3.98E-06
I240L	European	1/251402	3.98E-06
I240T	Most: Latino	5/251408	1.99E-05
V241M	European	4/282792	1.41E-05

I244V	Most: South Asian	12/251422	4.77E-05
R249C	European	1/251440	3.98E-06
R249H	Most: African	5/251434	1.99E-05
H250Y	European	3/251450	1.19E-05
H250R	European	1/251448	3.98E-06
N253G	European	1/251444	3.98E-06
L257V	Most: Latino	9/251444	3.58E-05
R258C	Most: European	7/251434	2.78E-05
R258H	European	4/251428	1.59E-05
T259A	South Asian	1/251410	3.98E-06
T259S	Other	1/251436	3.98E-06
R260W	Most: African	2/251438	7.96E-06
R260P	European	3/251428	1.19E-05
R260Q	Most: African	2/251428	7.95E-06
L262V	Most: European	20/282828	7.07E-05
G264S	Most: European	489/282814	1.73E-03
L265V	European	1/251426	3.98E-06
Q268H	South Asian	1/251432	3.98E-06
N274D	Other	1/251408	3.98E-06
L278F	South Asian	1/251388	3.98E-06
T287A	Most: European	1594/282558	5.64E-03
K289R	Latino	1/251176	3.98E-06
I290T	European	1/31404	3.18E-05
R292G	European	1/251148	3.98E-06
A295T	African	4/251044	1.59E-05
L297P	African	13/282450	4.60E-05
L301F	South Asian	1/250832	3.99E-06
A308T	African	1/251384	3.98E-06
A308S	African	17/282782	6.01E-05
A308G	African	1/251378	3.98E-06
I311V	South Asian	1/251372	3.98E-06
R312W	Most: East Asian	2/251360	7.96E-06
R312Q	Most: European	6/251358	2.39E-05
F315C	East Asian	1/251346	3.98E-06
R319Q	Most: European	4/251264	1.59E-05
L323W	African	1/251368	3.98E-06
L326S	South Asian	1/251388	3.98E-06
L326F	European	1/251370	3.98E-06
T336P	Most: European	3/282810	1.06E-05

D348V	European	3/250000	1.20E-05
D348A	South Asian	1/250000	4.00E-06
T349I	Most: South Asian	6/250090	2.40E-05
V350L	South Asian	1/250192	4.00E-06
V351I	East Asian	6/281672	2.13E-05
T352N	Latino	3/250484	3.99E-06
A354V	European	2/250484	3.99E-06
C355R	Ashkenazi Jewish	1/250634	3.99E-06
T365P	Latino	1/250100	4.00E-06
T365S	European	1/249958	4.00E-06
T365I	African	1/249958	4.00E-06
R366W	Most: European	2/281028	7.12E-06
R366Q	Most: Ashkenazi Jewish	3/249618	1.20E-05
R368W	Most: African	12/249298	4.81E-05
R370Q	European	3/248394	1.21E-05
E373A	South Asian	7/247376	2.83E-05

Supplementary Table S3 legend. RAD51 population variants from the Genome Aggregation Database (gnomad.broadinstitute.org) as of October 2021. Indicated are the mutation, population or most common population the variant is identified in, the variant allele count, and the total frequency. Note: “European” excludes individuals of Finnish descent. A126T and T287A have been observed in homozygous individuals (see **Table 2**), as has G264S.

Supplementary Table S4. RAD51C variant predictions.

Mutation*	PolyPhen-2 (1, ≥0.957)	SIFT (1, <0.05)	PROVEAN (1, ≤-2.5)	Total Score
Q11R	0 (0.93)	1 (0.023)	0 (-1.33)	1
R12W	1 (1.00)	1 (0.03)	1 (-3.82)	3
P21A	0 (0.067)	0 (0.184)	1 (-3.68)	1
P21S	0 (0.054)	1 (0.04)	1 (-4.01)	2
K26M	1 (0.998)	1 (0.001)	1 (-4.14)	3
L27P	1 (1.00)	1 (0.001)	1 (-5.1)	3
A30E	1 (0.999)	1 (0.002)	1 (-3.63)	3
P43S	0 (0.467)	0 (0.124)	1 (-3.89)	1
L91F	1 (0.995)	1 (0.027)	1 (-3.6)	3
F103V	1 (0.993)	0 (0.129)	1 (-5.26)	2
D108Y	1 (1.00)	1 (0.001)	1 (-8.67)	3
G112V	1 (1.00)	1 (0.001)	1 (-8.5)	3
G113S	1 (1.00)	1 (0.00)	1 (-5.97)	3
T121R	1 (1.00)	1 (0.001)	1 (-5.96)	3
G125S	1 (1.00)	1 (0.00)	1 (-5.98)	3
G125V	1 (1.00)	1 (0.00)	1 (-8.96)	3
A126T#	0 (0.066)	0 (0.144)	0 (-1.77)	0
G130A	1 (1.00)	1 (0.00)	1 (-5.98)	3
T132P	1 (1.00)	1 (0.00)	1 (-5.98)	3
Q133K	1 (1.00)	1 (0.00)	1 (-3.99)	3
C135R	1 (0.999)	0 (0.061)	1 (-6.48)	2
C135Y	1 (1.00)	1 (0.025)	1 (-6.12)	3
M136L#	0 (0.006)	0 (0.196)	0 (-1.09)	0
L138F	1 (0.995)	1 (0.003)	1 (-3.59)	3
V140G	1 (0.986)	1 (0.00)	1 (-6.39)	3
D141G	0 (0.885)	0 (0.2)	1 (-4.11)	1
Q143R	0 (0.943)	1 (0.004)	1 (-3.25)	2
I144T#	0 (0.885)	0 (0.078)	1 (-3.45)	1
G153D	1 (1.00)	1 (0.001)	1 (-6.34)	3
G153S	1 (0.999)	1 (0.006)	1 (-5.34)	3
D159N	1 (1.00)	1 (0.00)	1 (-4.65)	3
G162E	1 (1.00)	1 (0.002)	1 (-7.2)	3
G162R	1 (1.00)	1 (0.002)	1 (-7.17)	3
R212C#	1 (1.00)	1 (0.001)	1 (-7.2)	3
R214C#	0 (0.001)	0 (0.28)	0 (-1.52)	0
L219S#	1 (1.00)	1 (0.016)	1 (-3.49)	3
Y224H	0 (0.001)	0 (0.247)	0 (1.14)	0
L226P	1 (1.00)	1 (0.001)	1 (-6.23)	3
P247L	0 (0.109)	0 (0.302)	1 (-3.8)	1
R249C#	1 (1.00)	1 (0.00)	1 (-6.7)	3
R249H	1 (0.967)	1 (0.00)	1 (-4.16)	3
L257V#	0 (0.238)	0 (0.06)	0 (-1.99)	0
R258H**	1 (1.00)	1 (0.00)	1 (-4.13)	3
R260W#	1 (1.00)	1 (0.001)	1 (-5.73)	3
L262V#	0 (0.883)	1 (0.042)	0 (-2.38)	1
A279V	0 (0.883)	1 (0.044)	1 (-3.03)	2
T287A#	1 (0.988)	1 (0.00)	1 (-4.12)	3
A308S#	0 (0.771)	0 (0.308)	0 (-1.78)	0
A308T	1 (0.992)	1 (0.004)	1 (-2.71)	3
R312W#	1 (1.00)	1 (0.00)	1 (-6.9)	3
D318E	0 (0.001)	0 (1.00)	0 (0.75)	0
A324T	1 (0.981)	1 (0.03)	1 (-2.98)	3
P330H	1 (0.997)	1 (0.00)	1 (-7.17)	3
T336P	0 (0.767)	1 (0.026)	1 (-2.52)	2
E360Q	0 (0.596)	0 (0.196)	0 (-0.37)	0
R366Q	1 (0.998)	1 (0.031)	0 (-0.70)	2

Supplementary Table S4. *RAD51C* variants were scored for functional consequences using three predictive tools, Polymorphism Phenotyping version 2 (PolyPhen-2), Sorting Intolerant From Tolerant (SIFT), and Protein Variation Effect Analyzer (PROVEAN). For PolyPhen-2, ≥ 0.957 is considered probably damaging, while < 0.957 is considered possibly damaging or benign. SIFT uses a binary cutoff in which < 0.05 is damaging, while ≥ 0.5 is tolerated. PROVEAN also uses a binary cutoff, in this case ≤ -2.5 is considered deleterious, while > -2.5 is considered neutral. The predictive score in the last column is the sum of the of the binary scores used for the three predictive tools.

PolyPhen-2: <http://genetics.bwh.harvard.edu/pph2/bgi.shtml>

SIFT: <https://sift.bii.a-star.edu.sg>

PROVEAN: http://provean.jcvi.org/protein_batch_submit.php?species=human

Supplementary Table S5. RAD51C variants identified in ovarian and breast cancer patients in this study.

A.

RAD51C missense	NM_058216 change	Patient	Allele origin	Tumor VAF	Age	Diagnosis	Post-surgery	Chemotherapy	Survival
T132P	c.394A>C	1	germline	0.80	57	Stage IIIC HGSPPC	no visible disease	Cisplatin/Taxol	>10 years
Q133K	c.397C>A	1	germline	0.69	70	Stage IIIB HGSOC	residual disease <1cm	Carboplatin/Taxol	11 years
	c.397C>A	2	germline	no sample	45	Stage II HGSC		Carboplatin/Taxol	relapse 3 months
R312W	c.934C>T	1	germline	1.00	58	Stage IIIC HGSOC	no residual disease	Carboplatin/Taxol	>10 years
	c.934C>T	2	somatic	0.67	47	Stage III OC	metastatic	Carboplatin/Taxol	17 years
G130A	c.389G>C	1	somatic	0.54	32	Stage III BRCA	no residual disease	Adriamycin/Cycloph. Taxol/Carboplatin	>3 years

B.

Sample ID	BROCA Version	Source	Gene	Chromosome (hg19)	HGVS DNA Reference	HGVS Protein Reference	Variant Type	Predicted Effect	dbSNP/dbVar ID	Genotype	Allele Frequency	Target Coverage
T121R												
OCRFHG2724G	HRv3	Germline	RAD51C	chr17:56772508	c.362C>G	p.T121R	substitution	pathogenic	NA	NA	0%	258
	HRv3	Germline	BRCA2	chr13:32914172	c.5681dupA	p.Tyr1894Terfs	indel	pathogenic	rs80359527	NA	0%	336
	HRv3	Germline	TP53	chr17:7577114	c.824G>A	p.C275Y	substitution	pathogenic	rs863224451	NA	0%	241
OCRFHG2724T	HRv3	Tumor	RAD51C	chr17:56772508	c.362C>G	p.T121R	substitution	pathogenic	NA	heterozygous	24%	196
	HRv3	Tumor	BRCA2	chr13:32914172	c.5681dupA	p.Tyr1894Terfs	indel	pathogenic	rs80359527	heterozygous	33%	272
	HRv3	Tumor	TP53	chr17:7577114	c.824G>A	p.C275Y	substitution	pathogenic	rs863224451	homozygous	54%	267
Q133K												
OCRFHG2986G	HRv3	Germline	RAD51C	chr17:56772543	c.397C>A	p.Q133K	substitution	pathogenic	rs387907159	heterozygous	53%	235
OCRFHG2986T	HRv3	Tumor	RAD51C	chr17:56772543	c.397C>A	p.Q133K	substitution	pathogenic	rs387907159	homozygous	69%	194
OCRFHG2986T	HRv3	Tumor	TP53	chr17:7577081	c.857A>G	p.E286G	substitution	pathogenic	rs1057519985	homozygous	53%	156
WHMayo.056	HRv5	Germline	RAD51C	chr17:56772543	c.397C>A	p.Q133K	substitution	pathogenic	rs387907159	heterozygous	46%	198
WHMayo.055	HRv5	Germline	RAD51C	chr17:56772543	c.397C>A	p.Q133K	substitution	pathogenic	rs387907159	heterozygous	45%	152
R312W												
JML.NCI.1356	HRv6	Tumor	RAD51C	chr17:56801430	c.934C>T	p.R312W	substitution	pathogenic	rs730881932	homozygous	100%	348
	HRv6	Tumor	TP53	chr17:7578503	c.427delG	p.Val143Cysfs	indel	pathogenic	NA	homozygous	96%	158
MayoEO.6560	HRv6	Tumor	RAD51C	chr17:56801430	c.934C>T	p.R312W	substitution	pathogenic	rs730881932	homozygous	67%	349
	HRv6	Tumor	TP53	chr17:7574003	c.1024C>T	p.R342X	substitution	pathogenic	rs730882029	homozygous	45%	112

C.

Sample	Mean Target Coverage	Total Reads (passed filter)	Total Aligned Reads	Percent Reads On Bait	Percent Usable Bases on Target	Percent Duplication	Estimated Library Size
T121R							
OCRFHG2724T	160.1	7,918,094	7,408,430	41.6%	34.9%	2.7%	73,406,094
OCRFHG2724G	152.5	7,435,126	7,205,662	42.5%	35.4%	3.7%	49,332,874
Q133K							
OCRFHG2986G	230.0	NA	NA	NA	NA	NA	NA
OCRFHG2986T	194.0	NA	NA	NA	NA	NA	NA
WHM Mayo.056	174.0	NA	NA	NA	NA	NA	NA
WHM Mayo.055	216.0	NA	NA	NA	NA	NA	NA
R312W							
JML.NCI.1356	227.8	8,405,902	7,933,091	64.9%	53.2%	17.4%	10,360,722
MayoEO.6560	158.2	5,954,058	5,518,311	62.7%	52.1%	4.5%	31,933,614

Supplementary Table S5. RAD51C variants identified in ovarian and breast cancer patients in this study.

A. RAD51C variants identified in ovarian cancer patients through BROCA sequencing. Tumor DNA was not sequenced for Q133K mutation Patient 2 so that the variant allele frequency (VAF) could not be determined. The age at diagnosis is indicated. The patient with the T132P variant has been previously reported. In addition, the somatic variant G130A was identified in a triple negative breast cancer patient through MSK clinical sequencing. In this case, tumor purity was 50%; LOH is indicated due to the low tumor purity confirmed by the presence of a TP53 mutation (Q53*) at a VAF of 0.32.

B. BROCA sequencing results. The BROCA versions used are indicated (HRv3, HRv5, HRv6).

C. Sequencing quality control.